
TabImpute: Universal Zero-Shot Imputation for Tabular Data

Jacob Feitelberg¹ Dwaipayan Saha¹ Kyuseong Choi² Zaid Ahmad³ Anish Agarwal¹ Raaz Dwivedi⁴

Abstract

Missing data is a widespread problem in tabular settings. Existing solutions range from simple averaging to complex generative adversarial networks, but due to each method’s large variance in performance across real-world domains and time-consuming hyperparameter tuning, no universal imputation method exists. This performance variance is particularly pronounced in small datasets, where the models have the least amount of information. Building on TabPFN, a recent tabular foundation model for supervised learning, we propose TabImpute, a pre-trained transformer that delivers accurate and fast zero-shot imputations, requiring no fitting or hyperparameter tuning at inference time. To train and evaluate TabImpute, we introduce (i) an entry-wise featurization for tabular settings, enabling a 100× speedup over the previous TabPFN imputation method, (ii) a synthetic training data generation pipeline incorporating a diverse set of missingness patterns to enhance accuracy on real-world missing data problems, and (iii) MissBench, a comprehensive benchmark with 42 OpenML tables and 13 new missingness patterns. MissBench spans domains such as medicine, finance, and engineering, showcasing TabImpute’s robust performance compared to numerous established imputation methods.

1. Introduction

Missing data is ubiquitous across tabular datasets, affecting statisticians, economists, health officials, and businesses. For example, healthcare datasets may lack some rerecorded blood pressure measurements, or datasets merged from multiple sources may share only features. Regardless of

the source, missing data must usually be imputed to numerical values before employing statistical or machine learning models. Imputation methods range from simple approaches (e.g., constant values and averages) to more sophisticated techniques such as nearest-neighbor methods (Batista & Monard, 2003), matrix factorization methods such as SoftImpute (Hastie et al., 2015), and random forest regression, notably the MissForest algorithm (Stekhoven & Bühlmann, 2011). However, each method in the literature is typically tailored for specific settings, with performance varying significantly across datasets, domains, and missingness patterns (Van Buuren, 2012; Jarrett et al., 2022; Agarwal et al., 2023; Ibrahim et al., 2005). Building on recent advances in tabular representation learning (Hollmann et al., 2023; Ye et al., 2025), we propose a pre-trained transformer specifically designed for the tabular missing-data problem that produces accurate and fast zero-shot imputations.

(Rubin, 1976) proposed analyzing missingness based on its relationship with the data-generating process to determine whether missingness biases downstream estimation. Rubin demonstrated that when missingness is independent of the underlying data, the observed data distribution provides an unbiased basis for estimation. This framework categorizes missingness into three classes: Missing Completely At Random (MCAR), Missing At Random (MAR), and Missing Not At Random (MNAR) (Van Buuren, 2012; Sportisse et al., 2020a;b). MCAR defines scenarios where missingness occurs uniformly and independently of all data values. MAR encompasses cases where missingness depends on observed variables that can be appropriately conditioned upon during analysis. MNAR describes situations where missingness depends on unobserved factors that cannot be easily conditioned on.

While Rubin’s framework characterizes how missingness relates to the underlying data-generating process, it largely treats the missingness indicators for each variable as conditionally independent across entries. Recent work on structured missingness argues that, especially in large-scale multi-source datasets, missingness itself can exhibit rich multivariate structure that is not captured by the standard MCAR/MAR/MNAR taxonomy. In particular, (Mitra et al., 2023) introduces structured missingness as an umbrella term for mechanisms in which missingness follows systematic patterns. (Jackson et al., 2023) provides a com-

¹Industrial Engineering & Operations Research, Columbia University, New York, USA ²Statistics & Data Science, Cornell Tech, New York, USA ³Department of Statistics, Columbia University, New York, USA ⁴Operations Research & Information Engineering, Cornell Tech, New York, USA. Correspondence to: Jacob Feitelberg <jef2182@columbia.edu>.

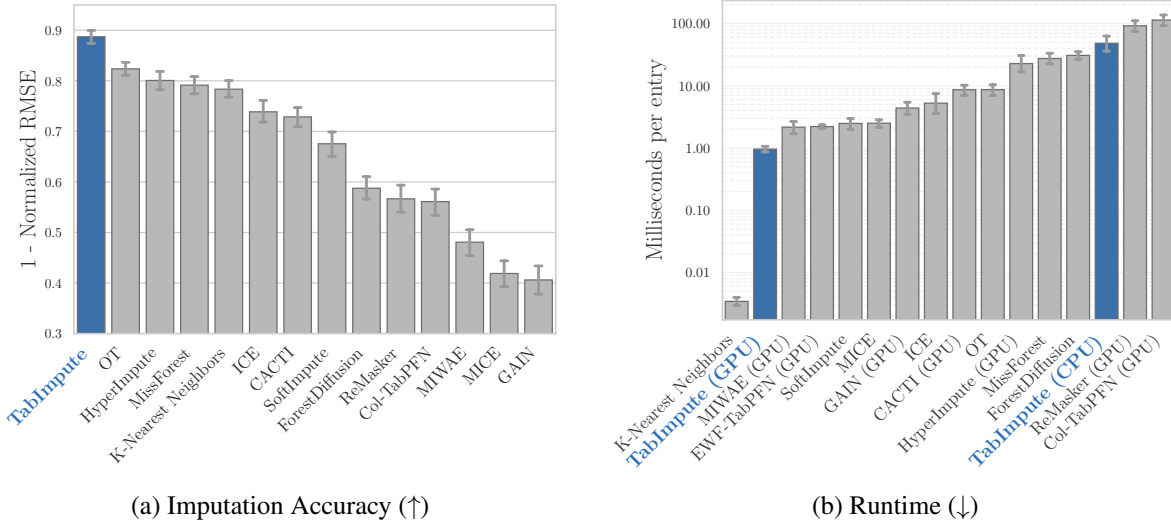


Figure 1. **Evaluation on real-world OpenML small datasets: MissBench.** We compare TabImpute with 13 other popular methods on MissBench. In panel (a), we plot the imputation accuracy (defined as 1 - normalized RMSE), which is calculated for each method, normalized within a dataset, and averaged across datasets and 13 missingness patterns. Accuracy scores are normalized to 0-1, with higher values better. Error bars indicate 95% confidence intervals. In panel (b), we compare the runtime per table entry. Any method not labeled (GPU) is tested on a CPU because it is not implemented on GPUs. See Sec. 3 for our exact computing specifications and Sec. 4 for accuracy score methodology.

plementary characterization that accounts for dependencies among missingness indicators across variables. We incorporate structured missingness by testing on 11 MNAR patterns.

Previous work typically introduced new missingness patterns within these categories and proposed pattern-specific solutions. For instance, (Agarwal et al., 2023) proposed a nearest neighbor-based matrix completion method specifically designed for a block-wise MNAR pattern. We instead develop a single method to perform well across diverse patterns and data domains by building on TabPFN, a popular tabular foundation model for supervised learning.

TabPFN is a pre-trained transformer model for supervised learning that performs well without any fine-tuning (Hollmann et al., 2025). The team behind TabPFN created an imputation method in their `tabpfn-extensions` Python package by using the TabPFN model in iterative column-wise imputation, denoted here as Col-TabPFN (available on GitHub¹). However, when evaluated on our new benchmark MissBench, consisting of 42 real-world small OpenML datasets and 13 missingness patterns, Col-TabPFN’s imputation approach shows low accuracy and slow runtime. We improve on this approach by introducing a new entry-wise featurization (EWF), allowing parallel prediction of each missing value using TabPFN’s model,

¹https://github.com/PriorLabs/tabpfn-extensions/blob/main/src/tabpfn_extensions/unsupervised/unsupervised.py

denoted EWF-TabPFN. To improve on EWF-TabPFN, we train a new underlying model specifically designed for tabular data imputation, TabImpute, to better fit this class of tasks, achieving the results shown in Fig. 1 and Tab. 1.

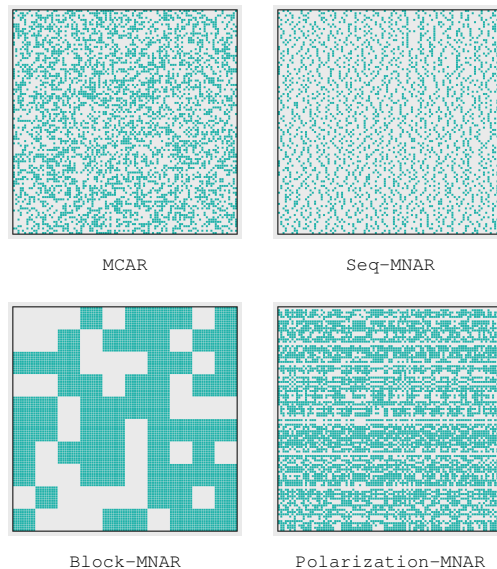


Figure 2. **Selection of synthetic missingness patterns implemented in MissBench.** Blue entries indicate observed values, and gray entries are unobserved.

The main contributions of this work can be summarized as follows (also shown in Fig. 3):

- We propose a new state-of-the-art pre-trained transformer model, TabImpute, for missing data imputation in small tables by building on TabPFN and introducing a new entry-wise missing data featurization (see Sec. 3 for details).
- We develop a synthetic data generation pipeline to create training datasets with a comprehensive collection of missing values covering a wide range of realistic MNAR patterns (see Sec. 3.1, Sec. A.2, and Tab. 10 for details).
- We demonstrate TabImpute’s performance on a novel, comprehensive test bench of small tables, which we call MissBench, using 42 real-world small OpenML datasets and 13 missingness patterns (see Sec. 4 for details) spanning many fields including biology, medicine, finance, and education.

Our code and implementation details for all our contributions above can be accessed on GitHub.²

1.1. Previous Work

We primarily build on missing-data imputation and tabular representation learning (TRL). While missing-data imputation is well-studied, with established theory dating back to the 1970s (Rubin, 1976), TRL using tabular foundation models is relatively new (Müller et al., 2022; Zhang et al., 2025; Hollmann et al., 2023; 2025). Below, we describe relevant work.

Imputation methods. Given the widespread nature of missing data, numerous imputation techniques have been proposed. These include averages, linear models over columns (Efron, 1994), random forest models (Hindy et al., 2024), ensemble methods (Jarrett et al., 2022), nearest neighbor-based methods (Chin et al., 2025), and even using generative adversarial networks (Yoon et al., 2018). For fully numerical data, matrix completion methods like SoftImpute (Hastie et al., 2015) have also been employed.

HyperImpute (Jarrett et al., 2022) combines the power of multiple classical imputation methods through iterative imputation (IM). IM loops over each column, using other columns to predict missing values until convergence. HyperImpute optimizes the imputer at each iteration over candidate methods, including MICE (Royston & White, 2011), SoftImpute (Hastie et al., 2015), column mean, MissForest (Stekhoven & Bühlmann, 2011), and Optimal Transport (Muzellec et al., 2020).

Tabular representation learning. Tabular representation learning focuses on building models that can gen-

eralize across diverse tabular domains. The pioneering work in this area is TabPFN, proposed in (Hollmann et al., 2023) and improved in (Hollmann et al., 2025). Since TabPFN’s introduction, numerous variants have emerged to address scalability and performance limitations, as well as further work aimed at clarifying its internal representations (Zhang et al., 2025; Ye et al., 2025). Recent advances include TabICL (Qu et al., 2025), a scalable foundation model that extends supervised learning capabilities to datasets with up to 500K samples through a novel two-stage architecture with column-then-row attention mechanisms. Other notable models include MITRA (Zhang & Robinson, 2025), a tabular foundation model pre-trained on purely synthetic data from a mix of random classifiers/regressors, and Toto (Cohen et al., 2025), which is optimized for time series forecasting on observability metrics. Additionally, CausalFM (Ma et al., 2025) enables Bayesian causal inference through structural causal model priors similar to TabPFN, while DO-PFN (Robertson et al., 2025) extends the PFN framework to estimate counterfactual distributions from observational data.

2. Background on Prior-data Fitted Networks and TabPFN

Prior-data Fitted Networks (PFNs) are a class of models that learn to approximate Bayesian inference for a given prior (Müller et al., 2022). Instead of fitting a new model from scratch, a PFN is an individual, large pre-trained Transformer to perform classification or regression in a single forward pass. This process, known as in-context learning (ICL), allows the model to make predictions using sequences of labeled examples provided directly in the input, without requiring any gradient updates (Dong et al., 2024). The entire prediction algorithm is contained in the weights of the network, which is trained once on millions of synthetically generated datasets sampled from the prior. At inference time, the trained PFN takes a real-world dataset, composed of training and test samples, as a set-valued input and returns a distribution over the output space. This output space is categorical for classification tasks and the real line for regression tasks.

Posterior predictive modeling. PFNs are rooted in Bayesian supervised learning, where the primary objective is to model the posterior predictive distribution (PPD) (MacKay, 1992; Seeger, 2004; Blei et al., 2017). Since computing the PPD is often intractable (MacKay, 1992), PFNs instead learn to approximate the PPD offline through a process called synthetic prior fitting (Müller et al., 2022). This is achieved using a prior specified by a sampling scheme that first samples a data-generating mechanism, $\phi \sim p(\phi)$, and then samples a synthetic dataset, $D \sim p(D|\phi)$. This process is repeated to generate millions

²<https://github.com/jacobf18/tabular>

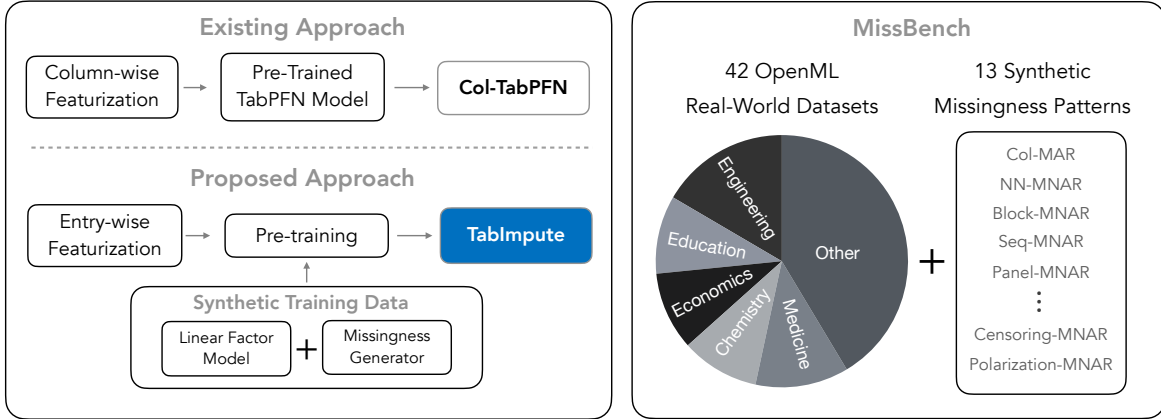


Figure 3. **Overview of our contributions.** The first row demonstrates Col-TabPFN, which performs iterative column-by-column imputation. We build on this by introducing an entry-wise featurization, as shown in the second row. We create a new synthetic data-generator for missingness data to train our model, TabImpute, shown in green (Sec. 3.1 and Sec. 3.2, respectively). We evaluate all the imputers on the comprehensive and rich set of OpenML datasets with many missingness patterns applied (Sec. 4).

of diverse datasets for training. The network’s parameters, θ , are then optimized to predict held-out test samples ($D_{\text{test}} \subset D$) conditioned on the rest of the dataset ($D_{\text{train}} = D \setminus D_{\text{test}}$). The training objective is to minimize the negative log likelihood (NLL) loss on these held-out examples: $\mathcal{L}(\theta) = \mathbb{E}_{((x_{\text{test}}, y_{\text{test}}) \cup D_{\text{train}}) \sim p(D)} [-\log q_{\theta}(y_{\text{test}} | x_{\text{test}}, D_{\text{train}})]$. Minimizing this loss ensures that the trained neural network q_{θ} approximates the true Bayesian PPD for the specified prior.

TabPFN. TabPFN is a PFN built specifically for tabular supervised learning (Hollmann et al., 2023). The model employs a novel two-way attention mechanism specifically designed for tabular data. The architecture uses alternating attention patterns: each cell first attends to other features within its row (inter-feature attention), then attends to the same feature across all rows (inter-sample attention). This design ensures permutation invariance for both samples and features while enabling efficient scaling to larger tables than those seen during training. TabPFN v2 (Hollmann et al., 2025) retains the core training paradigm of TabPFN v1 while introducing several key enhancements that improve accuracy, runtime, and applicability. Going forward, when referring to TabPFN, we mean TabPFN v2.

3. Pre-Training TabImpute on Synthetic Data

We pre-train the model on our novel missing-data prior using entry-wise featurization, both detailed below. Training used 8 H200 GPUs and an Intel Xeon Platinum 8592+ CPU over approximately 30 hours, processing 1.9 million synthetic tables, and evaluation used 1 H200 GPU. Our model matches TabPFN’s size and runs on CPU-only systems.

Entry-wise Featurization. Let X^* be the complete matrix with m rows and n columns, Ω be the set of missing entry indices, and X be the matrix with induced missingness: for each entry, $X_{ij} = X_{ij}^*$ if entry $(i, j) \notin \Omega$ (observed) and $X_{ij} = \star$ if $(i, j) \in \Omega$ (missing) where \star denotes a missing entry. Let $\Omega_{\text{obs}} = [m] \times [n] \setminus \Omega$. Each row of the entry-wise feature matrix is $(i \oplus j \oplus X_{i,:} \oplus X_{:,j})$ for entry $i, j \in [m] \times [n]$, where $X_{i,:}$ denotes the i -th row, $X_{:,j}$ the j -th column, and \oplus concatenation. Each row’s target is $y_{ij} = X_{ij}^*$. During pre-training, we train the model to predict target values for all $(i, j) \in \Omega$. This procedure creates a feature matrix of order $nm \times (n + m)$. This featurization captures all necessary information for each cell through its row and column context while enabling parallel computation of missing entries on GPUs. Although the input matrix size increases, the gains from parallelization outweigh this cost for small tables. Note that the features are created using the matrix with missing values X , not the true matrix X^* .

We demonstrate entry-wise featurization on a small toy matrix with missing values in Fig. 4. During pre-training, we have access to the true values of the NaNs in y . However, these values are only used to update the model’s weights via the loss function; the true values are never input into the model. The model internally handles NaN inputs by replacing their values with the column mean in the input matrix and then appending a binary matrix indicating which values are NaN. Internally, the NaN values in y are replaced with the mean of the non-NaN values (observed values) in y .

Architecture. Following TabPFN’s terminology, we refer to rows in the feature matrix with observed target values (non-NaN) as *input* points and rows with missing values

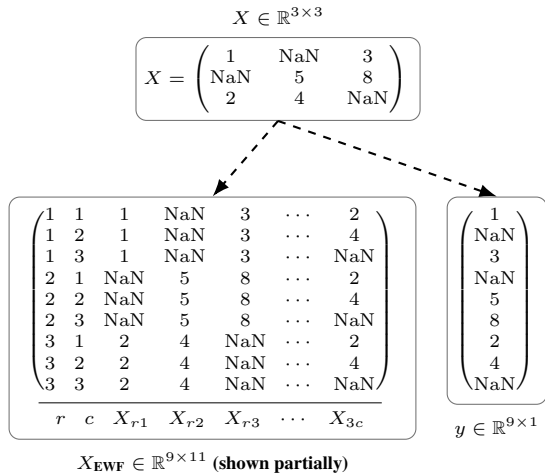


Figure 4. Entry-wise featurization to create a dataset pair (X_{EWF}, y) : each entry of the original matrix X produces one row in the feature matrix X_{EWF} , with the corresponding target $y_{(r,c)} = X_{r,c}$.

as *query* points. We adopt TabPFN’s base transformer architecture with one modification: we remove the attention mask that restricts information flow between query points. In the original supervised learning setting considered by TabPFN, this mask encodes an inductive bias that predictions for query points should be conditionally independent, reflecting the standard assumption that test points do not influence each other’s predictions. In contrast, in missing-data imputation, there is no assumption that missing entries (query points) should be independent. Indeed, under many missingness mechanisms, particularly non-MCAR settings, missing values may be strongly correlated through shared latent structure. Allowing query points to exchange information, therefore, better reflects the structure of the imputation problem.

3.1. Synthetic Training Data Generation

We generate around 1.9 million matrices with missing values to train our model through a two-step process: first, generating underlying data, then introducing missingness patterns on top.

3.1.1. DATA GENERATION: LINEAR FACTOR MODELS

We generate synthetic data using a linear factor model (LFM) (Bai & Ng, 2002). LFMs are commonly used in matrix completion literature to prove error bounds for matrix completion algorithms (Koren et al., 2009; Candes & Recht, 2012). This family of models generates a data matrix $Y \in \mathbb{R}^{m \times n}$ by assuming the data lies on or near a low-dimensional subspace. The simplest case generates the data matrix Y as the inner product of two lower-rank latent factor matrices, $U \in \mathbb{R}^{m \times k}$ and $V \in \mathbb{R}^{n \times k}$, where $k \ll n, m$ is the rank: $Y = UV^T$. The latent vectors (rows of U and

V) are sampled from a variety of distributions including Gaussian, Laplace, and Student’s-t.

During pre-training, we experimented with several classes of data-generating processes (DGPs), including matrices from nonlinear factor models and structural causal models (SCMs) similar to those in TabPFN. Training on SCM’s proved too computationally expensive, but we were able to train a model on nonlinear factor models. The model trained on linear factor models performed the best, as shown in Tab. 9 in Sec. A.4. We leave it as future work to explain why LFMs work so well in the small-table regime.

3.1.2. MISSINGNESS PATTERNS

After generating a complete data matrix $X^* \in \mathbb{R}^{m \times n}$, we introduce missingness by applying a mask $M \in \{0, 1\}^{m \times n}$, where the entry value $M_{ij} = 1$ if $(i, j) \in \Omega_{\text{obs}}$. To ensure TabImpute is robust and generalizable to the variety of ways data can be missing in real-world scenarios, we pre-train on millions of synthetic datasets, each with a different mask. For convenience, we define $p_{ij} = \mathbb{P}(M_{ij} = 1)$, the propensity of each entry. We evaluate TabImpute on 13 different missingness patterns: MCAR, 1 MAR pattern, and 11 MNAR patterns. For examples of these, see Fig. 2.

MCAR: MCAR missingness means the probability of an entry being missing, defined as its propensity, is constant across entries and independent from any other randomness. The missingness indicators M_{ij} are drawn i.i.d. from a Bernoulli distribution $M_{ij} \sim \text{Bern}(p)$ across all $(i, j) \in [m] \times [n]$ for some constant $p \in (0, 1)$. This is the simplest form of missingness, but is unrealistic (Van Buuren, 2012).

MAR: For MAR missingness, the probability of an entry being missing depends only on the observed values X . In other words, the randomness in MAR can be explained by conditioning on observed factors. Additionally, every entry has a positive probability of being observed (i.e., $p_{ij} > 0$). We simulate MAR through column-wise MAR, denoted Col-MAR: we choose several columns as predictor columns and use those values to mask entries in other columns. This is similar to the MAR approach taken in (Jarrett et al., 2022).

MNAR: For the most complex missingness class, MNAR, the probability of an entry being missing can depend on unobserved factors. Note that MNAR patterns are significantly more difficult to handle systematically, often requiring specialized methods for a specific kind of MNAR pattern (Van Buuren, 2012). Due to the flexibility of our entry-wise featurization, TabImpute can produce imputations for these highly complex scenarios. HyperImpute was tested on two MNAR patterns in the Appendix of (Jarrett et al., 2022), one where values are further masked after an MAR pattern and

another where values outside a certain range are masked. We build on this work by testing on 11 MNAR patterns (see Sec. A.2 and Tab. 10 for details). We implement a range of MNAR patterns to simulate plausible real-world scenarios. For example, we utilize the expressiveness of neural networks to create random propensity functions MNAR patterns, use bandit algorithms to induce column-adaptive missing patterns, simulate panel data missingness where some features are removed later, and censoring where sensor readings fall outside a detectable range.

3.2. Training TabImpute

We use the negative log likelihood (NLL) loss proposed in (Müller et al., 2022), and like other PFNs with continuous numerical output, we use the Riemann distribution output also proposed in (Müller et al., 2022). Since we can generate an unlimited amount of synthetic data, we do not reuse any synthetic data by using one gradient pass per batch of datasets. This allows our model to learn the underlying data-generating process and missingness mechanisms without risk of memorization. We use the AdamW optimizer (Loshchilov et al., 2017), a learning rate of 1e-4, a batch size of 16, and around 1.9 million synthetic datasets.

We trained TabImpute only on MCAR missingness, finding that this model generalized well to the other patterns without explicitly including them in training. In fact, we found that including other missingness patterns degraded overall performance. We had initially attempted to train the model sequentially on one missingness pattern at a time, but found that the network always experienced *catastrophic forgetting* (McCloskey & Cohen, 1989) irrespective of learning rate (i.e., it forgot how to handle the previous missingness patterns). After this, we attempted to mix several missingness types together: MCAR, MAR, and Self-MNAR. However, the model’s performance degraded overall because it focused only Self-MNAR. We attempted several techniques, including weighting schedules and GradNorm (Chen et al., 2018), a gradient normalization technique for multi-task learning, but found them unsuccessful in improving performance.

Why MCAR Pre-Training Generalizes Beyond MCAR.

By generating millions of synthetic datasets under MCAR, the model is exposed to a broad and diverse set of missingness masks. While MNAR mechanisms induce biased mask distributions that emphasize specific structural patterns, many such masks overlap with the support of masks encountered under MCAR generation, just with different frequencies. Importantly, TabImpute does not model the underlying missingness dynamics, but rather the conditional data distribution given the observed data, $P(X_{ij}|X_{\Omega_{\text{obs}}})$. This design is well suited for a general-purpose imputation method that maximizes predictive accuracy across many

missingness patterns without pattern-specific tuning. If the missingness mechanism is known a priori, though, specialized models perform much better, as shown in Tab. 3. Notably, our pipeline enables practitioners to easily train specialized models tailored to their missingness mechanisms without modifying the imputation algorithm.

4. Results on OpenML Datasets: MissBench

To evaluate TabImpute against other methods, we introduce MissBench: a missing-data imputation benchmark using 42 OpenML (Vanschoren et al., 2013) small tabular datasets with 13 synthetic missingness patterns. For every dataset and missingness pattern, we test each method’s ability to impute masked values. The 42 OpenML datasets span domains such as medicine, engineering, and education. The missingness patterns include MCAR, COLMAR, and 11 different MNAR patterns, with details provided in Sec. A.2. We test a suite of imputation methods on MissBench: SoftImpute (Hastie et al., 2015), MissForest (Stekhoven & Bühlmann, 2011), iterative chained estimators (ICE/MICE) (van Buuren & Groothuis-Oudshoorn, 2011; Royston & White, 2011), GAIN (Yoon et al., 2018), MIWAE (Mattei & Frellsen, 2019), an optimal transport-based method (Muzellec et al., 2020), ForestDiffusion (Jolicoeur-Martineau et al., 2024), ReMasker (Du et al., 2023), CACTI (Gorla et al., 2025), and Col-TabPFN (see Sec. 1).

We report results across all 42 datasets and 13 missingness patterns. Dataset sizes range from 50×5 to 170×55 . We evaluate only on datasets with numerical values without pre-existing missingness before applying synthetic patterns. Specific datasets are listed in Tab. 11 in Sec. A.4.

Imputation Accuracy. To ensure a fair comparison across datasets with different scales and inherent difficulties, we report an accuracy score normalized across datasets. For each dataset and missingness pattern, we first calculate the root mean squared error (RMSE) (standardized per column by mean and standard deviation) for every imputation method as $(\frac{1}{|\Omega|} \sum_{(i,j) \in \Omega} (X_{ij}^{\text{true}} - X_{ij}^{\text{imputed}})^2)^{1/2}$, where Ω denotes the set of missing entries. We then perform a min-max normalization on these RMSE scores across all methods within each dataset:

$$\text{Normalized RMSE} = \frac{\text{RMSE}_{\text{method}} - \min(\text{RMSE}_{\text{all}})}{\max(\text{RMSE}_{\text{all}}) - \min(\text{RMSE}_{\text{all}})}.$$

Finally, following the normalized negative RMSE metric used in (Hollmann et al., 2025), we define *Imputation Accuracy* as $1 - \text{Normalized RMSE}$, so that higher values indicate better performance, analogous to accuracy metrics where larger values correspond to improved predictions.

Table 1. Imputation Accuracy \pm Standard Error by Missingness Pattern. The number of samples used to calculate standard error are the number of datasets: 42.

Pattern	TabImpute	OT	HyperImpute	MissForest	K-Nearest Neighbors
MCAR	0.904 \pm 0.018	0.866 \pm 0.019	0.814 \pm 0.027	0.854 \pm 0.025	0.772 \pm 0.022
NN-MNAR	0.943 \pm 0.014	0.873 \pm 0.014	0.785 \pm 0.035	0.838 \pm 0.026	0.800 \pm 0.020
Self-MNAR	0.775 \pm 0.030	0.693 \pm 0.033	0.751 \pm 0.034	0.700 \pm 0.034	0.680 \pm 0.037
Col-MAR	0.921 \pm 0.018	0.788 \pm 0.032	0.868 \pm 0.029	0.830 \pm 0.025	0.872 \pm 0.017
Block-MNAR	0.937 \pm 0.013	0.857 \pm 0.027	0.854 \pm 0.027	0.850 \pm 0.024	0.893 \pm 0.014
Seq-MNAR	0.930 \pm 0.015	0.853 \pm 0.029	0.837 \pm 0.031	0.802 \pm 0.033	0.851 \pm 0.027
Panel-MNAR	0.955 \pm 0.008	0.918 \pm 0.011	0.883 \pm 0.031	0.897 \pm 0.019	0.940 \pm 0.011
Polarization-MNAR	0.825 \pm 0.025	0.787 \pm 0.021	0.631 \pm 0.039	0.580 \pm 0.033	0.658 \pm 0.028
Soft-Polarization-MNAR	0.805 \pm 0.047	0.773 \pm 0.029	0.669 \pm 0.036	0.625 \pm 0.039	0.635 \pm 0.035
Latent-Factor-MNAR	0.923 \pm 0.016	0.870 \pm 0.019	0.783 \pm 0.038	0.835 \pm 0.026	0.810 \pm 0.022
Cluster-MNAR	0.933 \pm 0.011	0.868 \pm 0.016	0.844 \pm 0.029	0.848 \pm 0.021	0.807 \pm 0.018
Two-Phase-MNAR	0.914 \pm 0.012	0.822 \pm 0.025	0.880 \pm 0.029	0.881 \pm 0.016	0.905 \pm 0.015
Censoring-MNAR	0.766 \pm 0.030	0.739 \pm 0.021	0.810 \pm 0.028	0.749 \pm 0.023	0.561 \pm 0.045
Overall	0.887 \pm 0.007	0.824 \pm 0.007	0.801 \pm 0.009	0.791 \pm 0.008	0.783 \pm 0.009

Tab. 1 presents results for each missingness pattern as well as overall performance. TabImpute achieves the best overall performance for nearly all individual patterns. For completeness, we list the performance of methods not shown in the table in Tab. 6 and non-normalized RMSE values in Tab. 12. TabImpute performs best under high missingness conditions (Fig. 5, Sec. A.1), which is expected since it leverages generative pre-training rather than relying solely on available dataset information like discriminative methods. In the Appendix, we report 1-Wasserstein distances in Tab. 7, report column-wise R^2 in Tab. 8, and test imputing categorical variables via one-hot encoding in Tab. 4.

For the other transformer-based methods, ReMasker (Du et al., 2023) and CACTI (Gorla et al., 2025), we observe lower relative performance than is reported in their papers. This difference is likely attributable to a regime mismatch: both methods are designed to operate on much larger tables. For example, Fig. 9 in (Du et al., 2023) shows ReMasker’s performance drops as dataset size decreases, eventually being overtaken by methods such as HyperImpute. Additionally, ReMasker is only tested on datasets with at least 308 rows and most having over 1,000 rows (Tab. 6 in (Du et al., 2023)), and CACTI is only tested on datasets with at least 3,539 rows and half having over 15,000 rows (Tab. A9 in (Gorla et al., 2025)). In Miss-Bench, however, we focus on small tables with at most 170 rows, resulting in a low-information setting. TabImpute is pre-trained to perform well with less information by leveraging its strong prior. These results highlight the difficulty of the small-table imputation problem and suggest that different imputation methods may be complementary across data regimes.

Discussion on Imputation Accuracy Metric. Choosing an imputation metric is challenging because: (i) columns

can have very different scales, (ii) datasets can have very different scales, and (iii) some datasets are inherently more difficult to impute than others (see Fig. 2 in (Jarrett et al., 2022)). As a result, there is no consensus in the literature on the preferred method for measuring imputation accuracy. For example, MissForest reports RMSE standardized by the mean and standard deviation of the entire table’s missing values (Hindy et al., 2024). HyperImpute reports non-standardized RMSE and column-wise 1-Wasserstein distance (Jarrett et al., 2022). CACTI reports RMSE, 1-Wasserstein distance, and column-wise R^2 (Gorla et al., 2025). In our evaluation, we standardize RMSE values at the column level, since columns can differ substantially in scale (e.g., income versus age).

Further, a subtle issue that can arise in imputation benchmarking is data leakage through normalization. In particular, the evaluation pipelines of ReMasker (Du et al., 2023) and HyperImpute (Jarrett et al., 2022) apply min-max scaling to each column *before* inducing missingness. So, if an extreme value is masked, the normalized value itself implicitly reveals information about the missing entry. To avoid data leakage, we standardize each column *after* inducing missingness.

Multiple imputation (MI) Metrics. In multiple imputation, a dataset is imputed multiple times independently to provide better confidence intervals of downstream quantities (Van Buuren, 2012). Given two imputation methods that have the same imputation accuracy, one would prefer a method with higher uncertainty to not provide false precision on imputed values (Van Buuren, 2012; Li et al., 2015; Jolicoeur-Martineau et al., 2024). We assess performance for multiple imputation by repeating imputation 5 times per entry and calculating the median absolute deviation (MAD), minimum RMSE, and average RMSE,

shown in Tab. 2 across the 5 samples per entry, following the methodology of ForestDiffusion (Jolicoeur-Martineau et al., 2024). While most methods require a full run to produce a new imputation, TabImpute outputs a distribution that can then be sampled from directly. Thus, multiple imputation for TabImpute runs as fast as single imputation.

TabImpute provides better diversity than methods of comparable imputation accuracy (MissForest and HyperImpute). The false precision of MissForest and HyperImpute is evident in their lower minimum RMSE values. Note that in Tab. 2, TabImpute has a higher average RMSE value than MissForest and HyperImpute. This is because TabImpute has greater diversity in its estimates (the samples have a larger spread). When comparing only the median-sample estimate, though, TabImpute has better accuracy, as shown in the first row of Tab. 1. Thus, TabImpute provides practitioners with the best of both worlds: If they require multiple imputation for uncertainty estimates, TabImpute provides diverse estimates, and if they require a single good imputation, TabImpute provides the most accurate estimate.

Table 2. Multiple Imputation Metrics: Per-Entry Metrics With 5 Samples Per Entry (MCAR, Probability of Missing = 0.4).

Method	MAD	Min. RMSE	Avg. RMSE
MICE	0.359 ± 0.002	0.264 ± 0.003	0.859 ± 0.005
MIWAE	0.267 ± 0.001	0.385 ± 0.005	0.927 ± 0.005
GAIN	0.200 ± 0.001	0.361 ± 0.004	0.789 ± 0.005
TabImpute	0.199 ± 0.002	0.337 ± 0.004	0.722 ± 0.006
ForestDiffusion	0.181 ± 0.001	0.291 ± 0.004	0.739 ± 0.005
ReMasker	0.138 ± 0.001	0.358 ± 0.004	0.648 ± 0.005
CACTI	0.100 ± 0.000	0.422 ± 0.003	0.639 ± 0.003
OT	0.049 ± 0.000	0.440 ± 0.005	0.547 ± 0.005
HyperImpute	0.037 ± 0.001	0.420 ± 0.004	0.551 ± 0.005
MissForest	0.036 ± 0.000	0.434 ± 0.005	0.532 ± 0.005
SoftImpute	0.001 ± 0.000	0.577 ± 0.005	0.649 ± 0.005
ICE	0.000 ± 0.000	0.606 ± 0.005	0.606 ± 0.005
K-Nearest Neighbors	0.000 ± 0.000	0.570 ± 0.005	0.570 ± 0.005

Specialized TabImpute Models. Here, we show the relative performance of three models trained on MCAR, Col-MAR, and Self-MNAR, respectively (see Tab. 3). The model trained on Self-MNAR performs much better than the other models on Self-MNAR, which is to be expected. However, it does not generalize well to other patterns because the masks generated by the Self-MNAR pattern do not cover the types of masks generated by other patterns. Interestingly, the MCAR-trained model performed slightly better on Col-MAR patterns than the model trained on Col-MAR exclusively. One possible hypothesis is that the masks generated under MAR pattern are well covered by MCAR masks, and MCAR masks produce a better underlying model. Note that the imputation accuracy scores are different for Tab. 1 and Tab. 3 because the MAR and Self-MNAR models are not included in the normalization in Tab. 1.

Table 3. Imputation Accuracy ± Standard Error by Missingness Pattern for Specialized TabImpute Models

Trained On ⇒	MCAR	Col-MAR	Self-MNAR
MCAR	0.938 ± 0.028	0.832 ± 0.024	0.020 ± 0.020
Self-MNAR	0.463 ± 0.067	0.329 ± 0.065	0.624 ± 0.072
Col-MAR	0.899 ± 0.042	0.811 ± 0.050	0.081 ± 0.041
Overall	0.766 ± 0.034	0.656 ± 0.035	0.243 ± 0.037

5. Conclusion & Future Work

In this paper, we present TabImpute, a pre-trained transformer for imputing missing data in small tables. We build on recent work in tabular representation learning by adapting TabPFN’s architecture and training pipeline for the missing data setting. Though TabImpute is trained purely on synthetic data, it accurately imputes entries on real-world OpenML data across a comprehensive set of missingness patterns, demonstrating its ability to generalize to unseen domains. We open-source not only our model architecture and weights, but also our training and evaluation code. We hope this will facilitate others in validating, utilizing, and building upon our work.

While TabImpute performs well on small tables, it is not designed for very large tables because of the entry-wise featurization and quadratic attention cost. However, since we use the same network architecture as TabPFN, any further improvements to TabPFN’s architecture can be ported to TabImpute immediately. For example, (Zeng et al., 2025) and (Qu et al., 2025) propose different attention mechanisms to speed up TabPFN-like architectures for tabular data.

In future work, we plan on (i) exploring training further on more complex missingness patterns and data-generating processes, (ii) enhancing our method to impute categorical data better, (iii) extending our evaluation set to causal-inference settings, which can be modeled as missing-data problems (Agarwal et al., 2023), and (iv) improving the architecture to scale to larger datasets.

Impact statement. Our work seeks to advance the fields of machine learning and data science by improving missing-data imputation. While there are many possible impacts on society as a whole from our work, we do not feel that any direct impacts on society need to be highlighted here.

References

- Agarwal, A., Dahleh, M., Shah, D., and Shen, D. Causal matrix completion. In *The thirty sixth annual conference on learning theory*, pp. 3821–3826. PMLR, 2023.
- Auer, P., Cesa-Bianchi, N., and Fischer, P. Finite-time analysis of the multiarmed bandit problem. *Machine learning*, 47(2):235–256, 2002.
- Bai, J. and Ng, S. Determining the number of factors in approximate factor models. *Econometrica*, 70(1): 191–221, 2002. doi: <https://doi.org/10.1111/1468-0262.00273>. URL <https://onlinelibrary.wiley.com/doi/abs/10.1111/1468-0262.00273>.
- Batista, G. E. A. P. A. and Monard, M. C. An analysis of four missing data treatment methods for supervised learning. *Applied Artificial Intelligence*, 17(5-6):519–533, 2003. doi: 10.1080/713827181. URL <https://doi.org/10.1080/713827181>.
- Bethlehem, J. Selection bias in web surveys. *International statistical review*, 78(2):161–188, 2010.
- Blei, D. M., Kucukelbir, A., and McAuliffe, J. D. Variational inference: A review for statisticians. *Journal of the American statistical Association*, 112(518):859–877, 2017.
- Candes, E. and Recht, B. Exact matrix completion via convex optimization. *Communications of the ACM*, 55(6): 111–119, 2012.
- Cavari, A. and Freedman, G. Survey nonresponse and mass polarization: The consequences of declining contact and cooperation rates. *American Political Science Review*, 117(1):332–339, 2023.
- Chen, H., Quandt, S. A., Grzywacz, J. G., and Arcury, T. A. A bayesian multiple imputation method for handling longitudinal pesticide data with values below the limit of detection. *Environmetrics*, 24(2):132–142, 2013.
- Chen, Z., Badrinarayanan, V., Lee, C.-Y., and Rabinovich, A. Gradnorm: Gradient normalization for adaptive loss balancing in deep multitask networks. In *International conference on machine learning*, pp. 794–803. PMLR, 2018.
- Chin, C., Khubchandani, A., Maskara, H., Choi, K., Feitelberg, J., Gong, A., Paul, M., Sadhukhan, T., Agarwal, A., and Dwivedi, R. N²: A unified python package and test bench for nearest neighbor-based matrix completion. *arXiv preprint arXiv:2506.04166*, 2025.
- Cohen, B., Khwaja, E., Doubli, Y., Lemaachi, S., Lettieri, C., Masson, C., Miccinilli, H., Ramé, E., Ren, Q., Rostamizadeh, A., du Terrail, J. O., Toon, A.-M., Wang, K., Xie, S., Xu, Z., Zhukova, V., Asker, D., Talwalkar, A., and Abou-Amal, O. This time is different: An observability perspective on time series foundation models, 2025. URL <https://arxiv.org/abs/2505.14766>.
- Devlin, J., Chang, M.-W., Lee, K., and Toutanova, K. Bert: Pre-training of deep bidirectional transformers for language understanding. In *Proceedings of the 2019 conference of the North American chapter of the association for computational linguistics: human language technologies, volume 1 (long and short papers)*, pp. 4171–4186, 2019.
- Diaz-Ordaz, K., Kenward, M. G., Cohen, A., Coleman, C. L., and Eldridge, S. Are missing data adequately handled in cluster randomised trials? a systematic review and guidelines. *Clinical Trials*, 11(5):590–600, 2014.
- Dong, Q., Li, L., Dai, D., Zheng, C., Ma, J., Li, R., Xia, H., Xu, J., Wu, Z., Liu, T., Chang, B., Sun, X., Li, L., and Sui, Z. A survey on in-context learning, 2024. URL <https://arxiv.org/abs/2301.00234>.
- Du, T., Melis, L., and Wang, T. Remasker: Imputing tabular data with masked autoencoding. *arXiv preprint arXiv:2309.13793*, 2023.
- Efron, B. Missing data, imputation, and the bootstrap. *Journal of the American Statistical Association*, 89 (426):463–475, 1994.
- Enders, C. K., Mistler, S. A., and Keller, B. T. Multilevel multiple imputation: A review and evaluation of joint modeling and chained equations imputation. *Psychological methods*, 21(2):222, 2016.
- Fix, E. and Hodges, J. L. Discriminatory analysis. nonparametric discrimination: Consistency properties. *International Statistical Review / Revue Internationale de Statistique*, 57(3):238–247, 1989. ISSN 03067734, 17515823. URL <http://www.jstor.org/stable/1403797>.
- Ghosh, S., Kim, R., Chhabria, P., Dwivedi, R., Klasnja, P., Liao, P., Zhang, K., and Murphy, S. Did we personalize? assessing personalization by an online reinforcement learning algorithm using resampling. *Machine learning*, 113(7):3961–3997, 2024.
- Goodfellow, I., Pouget-Abadie, J., Mirza, M., Xu, B., Warde-Farley, D., Ozair, S., Courville, A., and Bengio, Y. Generative adversarial networks. *Communications of the ACM*, 63(11):139–144, 2020.
- Gorla, A., Wang, R., Liu, Z., An, U., and Sankararaman, S. Cacti: Leveraging copy masking and contextual information to improve tabular data imputation. *arXiv preprint arXiv:2506.02306*, 2025.

- Graham, J. W., Taylor, B. J., Olchowski, A. E., and Cum-
sille, P. E. Planned missing data designs in psychological
research. *Psychological methods*, 11(4):323, 2006.
- Hastie, T., Mazumder, R., Lee, J. D., and Zadeh, R. Matrix
completion and low-rank svd via fast alternating least
squares. *The Journal of Machine Learning Research*, 16
(1):3367–3402, 2015.
- Hausman, J. A. and Wise, D. A. Attrition bias in exper-
imental and panel data: the gary income maintenance
experiment. *Econometrica: Journal of the Econometric
Society*, pp. 455–473, 1979.
- Helsel, D. R. *Statistics for censored environmental data
using Minitab and R*, volume 77. John Wiley & Sons,
2011.
- Hindy, V., Vallelado, M. V., and Sep905. yuensh-
ingyan/missforest: Missforest in python - arguably
the best missing values imputation method, Au-
gust 2024. URL [https://doi.org/10.5281/
zenodo.13368883](https://doi.org/10.5281/zenodo.13368883).
- Hollmann, N., Müller, S., Eggensperger, K., and Hutter,
F. TabPFN: A transformer that solves small tabular
classification problems in a second. In *The Eleventh
International Conference on Learning Representations*,
2023. URL [https://openreview.net/forum?
id=cp5PvcI6w8_](https://openreview.net/forum?id=cp5PvcI6w8_).
- Hollmann, N., Müller, S., Purucker, L., Krishnakumar, A.,
Körfer, M., Hoo, S. B., Schirrmeyer, R. T., and Hut-
ter, F. Accurate predictions on small data with a tabular
foundation model. *Nature*, 637(8045):319–326, 2025.
- Hu, N., Zhang, J., and Pavlou, P. A. Overcoming the j-
shaped distribution of product reviews. *Communications
of the ACM*, 52(10):144–147, 2009.
- Ibrahim, J. G. and Molenberghs, G. Missing data methods
in longitudinal studies: a review. *Test*, 18(1):1–43, 2009.
- Ibrahim, J. G., Chen, M.-H., Lipsitz, S. R., and Her-
ring, A. H. Missing-data methods for generalized linear
models. *Journal of the American Statistical As-
sociation*, 100(469):332–346, 2005. doi: 10.1198/
016214504000001844. URL [https://doi.org/
10.1198/016214504000001844](https://doi.org/10.1198/016214504000001844).
- Jackson, J., Mitra, R., Hagenbuch, N., McGough, S., and
Harbron, C. A complete characterisation of structured
missingness, 2023. URL [https://arxiv.org/
abs/2307.02650](https://arxiv.org/abs/2307.02650).
- Jarrett, D., Cebere, B. C., Liu, T., Curth, A., and van der
Schaar, M. Hyperimpute: Generalized iterative im-
putation with automatic model selection. In *Internat-
ional Conference on Machine Learning*, pp. 9916–9937.
PMLR, 2022.
- Jin, H., Ma, Y., and Jiang, F. Matrix completion with co-
variate information and informative missingness. *Jour-
nal of Machine Learning Research*, 23(180):1–62, 2022.
- Jolicœur-Martineau, A., Fatras, K., and Kachman, T. Gen-
erating and imputing tabular data via diffusion and flow-
based gradient-boosted trees. In *International confer-
ence on artificial intelligence and statistics*, pp. 1288–
1296. PMLR, 2024.
- Karpievitch, Y., Stanley, J., Taverner, T., Huang, J., Ad-
kins, J. N., Ansong, C., Heffron, F., Metz, T. O., Qian,
W.-J., Yoon, H., et al. A statistical framework for protein
quantitation in bottom-up ms-based proteomics. *Bioin-
formatics*, 25(16):2028–2034, 2009.
- Koren, Y., Bell, R., and Volinsky, C. Matrix factorization
techniques for recommender systems. *Computer*, 42(8):
30–37, 2009. doi: 10.1109/MC.2009.263.
- Lattimore, T. and Szepesvári, C. *Bandit algorithms*. Cam-
bridge University Press, 2020.
- Lazar, C., Gatto, L., Ferro, M., Bruley, C., and Burger, T.
Accounting for the multiple natures of missing values in
label-free quantitative proteomics data sets to compare
imputation strategies. *Journal of proteome research*, 15
(4):1116–1125, 2016.
- Li, P., Stuart, E. A., and Allison, D. B. Multiple imputation:
a flexible tool for handling missing data. *Jama*, 314(18):
1966–1967, 2015.
- Little, R. J. Modeling the drop-out mechanism in repeated-
measures studies. *Journal of the american statistical as-
sociation*, 90(431):1112–1121, 1995.
- Little, R. J. and Rubin, D. B. *Statistical analysis with miss-
ing data*. John Wiley & Sons, 2019.
- Loshchilov, I., Hutter, F., et al. Fixing weight decay regu-
larization in adam. *arXiv preprint arXiv:1711.05101*, 5
(5):5, 2017.
- Ma, Y., Frauen, D., Javurek, E., and Feuerriegel, S. Foun-
dation models for causal inference via prior-data fitted
networks, 2025. URL [https://arxiv.org/abs/
2506.10914](https://arxiv.org/abs/2506.10914).
- MacKay, D. J. A practical bayesian framework for back-
propagation networks. *Neural computation*, 4(3):448–
472, 1992.

- Marlin, B. M. and Zemel, R. S. Collaborative prediction and ranking with non-random missing data. In *Proceedings of the third ACM conference on Recommender systems*, pp. 5–12, 2009.
- Mattei, P.-A. and Frellsen, J. Miwae: Deep generative modelling and imputation of incomplete data sets. In *International Conference on Machine Learning*, pp. 4413–4423. PMLR, 2019.
- McCloskey, M. and Cohen, N. J. Catastrophic interference in connectionist networks: The sequential learning problem. In *Psychology of learning and motivation*, volume 24, pp. 109–165. Elsevier, 1989.
- Mitra, R., McGough, S. F., Chakraborti, T., Holmes, C., Copping, R., Hagenbuch, N., Biedermann, S., Noonan, J., Lehmann, B., Shenvi, A., et al. Learning from data with structured missingness. *Nature Machine Intelligence*, 5(1):13–23, 2023.
- Mohan, K. On handling self-masking and other hard missing data problems. In *AAAI Symposium 2018*, 2018.
- Moore, J. C. and Welniak, E. J. Income measurement error in surveys: A review. *Journal of official statistics*, 16(4): 331, 2000.
- Müller, S., Hollmann, N., Arango, S. P., Grabocka, J., and Hutter, F. Transformers can do bayesian inference. In *International Conference on Learning Representations*, 2022. URL <https://openreview.net/forum?id=KSugKcbNf9>.
- Muzellec, B., Josse, J., Boyer, C., and Cuturi, M. Missing data imputation using optimal transport. In *International Conference on Machine Learning*, pp. 7130–7140. PMLR, 2020.
- Neyman, J. Contribution to the theory of sampling human populations. *Journal of the American Statistical Association*, 33(201):101–116, 1938.
- Qu, J., Holzmüller, D., Varoquaux, G., and Morvan, M. L. Tabicl: A tabular foundation model for in-context learning on large data. *arXiv preprint arXiv:2502.05564*, 2025.
- Rhemtulla, M. and Hancock, G. R. Planned missing data designs in educational psychology research. *Educational Psychologist*, 51(3-4):305–316, 2016.
- Robertson, J., Reuter, A., Guo, S., Hollmann, N., Hutter, F., and Schölkopf, B. Do-pfn: In-context learning for causal effect estimation, 2025. URL <https://arxiv.org/abs/2506.06039>.
- Royston, P. and White, I. R. Multiple imputation by chained equations (mice): implementation in stata. *Journal of statistical software*, 45:1–20, 2011.
- Rubin, D. B. Inference and missing data. *Biometrika*, 63(3):581–592, 1976.
- Schnabel, T., Swaminathan, A., Singh, A., Chandak, N., and Joachims, T. Recommendations as treatments: Debiasing learning and evaluation. In *international conference on machine learning*, pp. 1670–1679. PMLR, 2016.
- Seeger, M. Gaussian processes for machine learning. *International journal of neural systems*, 14(02):69–106, 2004.
- Sportisse, A., Boyer, C., and Josse, J. Imputation and low-rank estimation with missing not at random data. *Statistics and Computing*, 30(6):1629–1643, 2020a.
- Sportisse, A., Boyer, C., and Josse, J. Estimation and imputation in probabilistic principal component analysis with missing not at random data. In Larochele, H., Ranzato, M., Hadsell, R., Balcan, M., and Lin, H. (eds.), *Advances in Neural Information Processing Systems*, volume 33, pp. 7067–7077. Curran Associates, Inc., 2020b. URL https://proceedings.neurips.cc/paper_files/paper/2020/file/4ecb679fd35dcfd0f0894c399590bela-Paper.pdf.
- Steck, H. Training and testing of recommender systems on data missing not at random. In *Proceedings of the 16th ACM SIGKDD international conference on Knowledge discovery and data mining*, pp. 713–722, 2010.
- Stekhoven, D. J. and Bühlmann, P. Missforest—non-parametric missing value imputation for mixed-type data. *Bioinformatics*, 28(1):112–118, 10 2011.
- Thompson, W. R. On the likelihood that one unknown probability exceeds another in view of the evidence of two samples. *Biometrika*, 25(3/4):285–294, 1933.
- Van Buuren, S. Multiple imputation of multilevel data. In *Handbook of advanced multilevel analysis*, pp. 173–196. Routledge, 2011.
- Van Buuren, S. *Flexible imputation of missing data*, volume 10. CRC press Boca Raton, FL, 2012.
- van Buuren, S. and Groothuis-Oudshoorn, K. Mice: Multivariate imputation by chained equations in r. *Journal of Statistical Software*, 45(3): 1–67, 2011. doi: 10.18637/jss.v045.i03. URL <https://www.jstatsoft.org/index.php/jss/article/view/v045i03>.

- Vanschoren, J., van Rijn, J. N., Bischl, B., and Torgo, L. Openml: Networked science in machine learning. *SIGKDD Explorations*, 15(2):49–60, 2013. doi: 10.1145/2641190.2641198. URL <http://doi.acm.org/10.1145/2641190.2641198>.
- Ye, H.-J., Liu, S.-Y., and Chao, W.-L. A closer look at tabpfn v2: Strength, limitation, and extension. *arXiv preprint arXiv:2502.17361*, 2025.
- Yoon, J., Jordon, J., and van der Schaar, M. Gain: Missing data imputation using generative adversarial nets. In *International Conference on Machine Learning (ICML)*, 2018.
- Zeng, Y., Dinh, T., Kang, W., and Mueller, A. C. Tabflex: Scaling tabular learning to millions with linear attention. *arXiv preprint arXiv:2506.05584*, 2025.
- Zhang, Q., Tan, Y. S., Tian, Q., and Li, P. Tabpfn: One model to rule them all?, 2025. URL <https://arxiv.org/abs/2505.20003>.
- Zhang, X. and Robinson, D. M. Mitra: Mixed synthetic priors for enhancing tabular foundation models, Jul 2025. URL <https://www.amazon.science/blog/mitra-mixed-synthetic-priors-for-enhancing-tabular-foundation-models>.

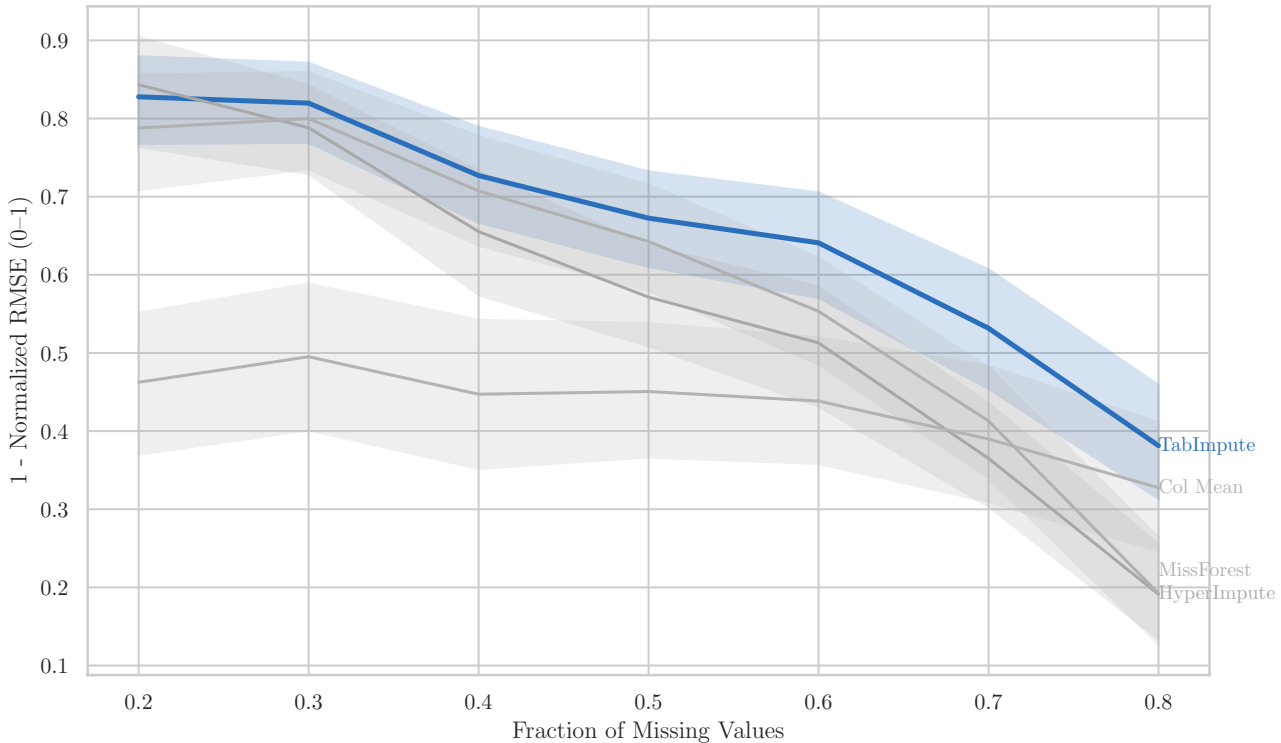


Figure 5. **Imputation Accuracy vs. probability of missingness for MCAR.** TabImpute performs the best when missingness is higher because it is a generative model that fits to the data in-context.

A. Appendix

Here we present the rest of the missingness patterns we tested on, tables with further results, the methods we tested against, and the OpenML datasets we evaluated on.

A.1. Additional tests

Next, we discuss when TabImpute does well and when HyperImpute and other methods do well. We found that an important factor in determining performance was the level of missingness. The probability of missingness can only be controlled precisely for MCAR. Thus, we show in Fig. 5 the performance of the top methods as we increase the missingness level.

Support for categorical variables. We support imputing categorical variables via one-hot encodings: First, we convert each categorical column into several one-hot encoding columns. Then, we impute missing entries within this now purely numerical matrix. We then choose the class with the highest score as the categorical imputation for that missing entry. Note that we could also perform a softmax operation over the imputed scores within the one-hot encoded columns to output probabilities over classes. With this method, TabImpute achieves AUC close to that of MissForest and HyperImpute when tested on MCAR missingness with the probability of missing set to 0.4, as shown in Tab. 4. We leave incorporating categorical features into the pre-training procedure for future work.

A.2. Details for MNAR Missingness Patterns

This section provides the mathematical and implementation details for each of the simulated MNAR missingness mechanisms that we implement and test. For each pattern, we define the mechanism by which the missingness mask M is generated, where $M_{ij} = 1$ if the value X_{ij} is observed and $M_{ij} = 0$ otherwise.

Table 4. Area Under the Curve (AUC) Performance on Categorical Columns with MCAR (Probability of Missing = 0.4) missingness.

OpenML Dataset	HyperImpute	MissForest	TabImpute	Mode
ChronicKidneyDisease	0.602	0.582	0.525	0.500
Dog Breeds Ranked	0.566	0.579	0.539	0.500
HappinessRank 2015	0.486	0.466	0.677	0.500
MY DB	0.480	0.514	0.521	0.500
Online Sales	0.790	0.809	0.869	0.500
Parkinson Dataset	0.665	0.640	0.523	0.500
acute-inflammations	0.761	0.756	0.723	0.500
aids	0.511	0.573	0.509	0.500
analcatacreditscore	0.678	0.672	0.491	0.500
analcatacyyoung8092	0.683	0.649	0.611	0.500
analcatacyyoung9302	0.713	0.700	0.629	0.500
analcataimpeach	0.751	0.749	0.706	0.500
analcatanaaa	0.549	0.547	0.500	0.500
analcatawildcat	0.749	0.682	0.674	0.500
auto price	0.749	0.802	0.761	0.500
backache	0.529	0.516	0.502	0.500
blogger	0.558	0.573	0.499	0.500
caesarian-section	0.534	0.499	0.518	0.500
cloud	0.436	0.409	0.440	0.500
cm1 req	0.677	0.658	0.602	0.500
cocomo numeric	0.629	0.618	0.655	0.500
conference attendance	0.500	0.512	0.499	0.500
corral	0.553	0.558	0.575	0.500
cpu	0.694	0.675	0.546	0.500
fl2000	0.608	0.468	0.533	0.500
flags	0.584	0.583	0.517	0.500
fruitfly	0.602	0.604	0.593	0.500
grub-damage	0.620	0.584	0.541	0.500
hutsof99 logis	0.569	0.568	0.583	0.500
iris	0.885	0.885	0.827	0.500
kidney	0.599	0.460	0.498	0.500
lowbwt	0.587	0.582	0.547	0.500
lung	0.558	0.483	0.496	0.500
lungcancer GSE31210	0.647	0.527	0.567	0.500
lymph	0.641	0.594	0.547	0.500
molecular-biology promoters	0.508	0.505	0.504	0.500
mux6	0.507	0.481	0.502	0.500
nadeem	0.594	0.521	0.542	0.500
nasa numeric	0.596	0.594	0.561	0.500
postoperative-patient-data	0.468	0.494	0.496	0.500
prnn crabs	0.840	0.687	0.737	0.500
prnn viruses	0.563	0.588	0.551	0.500
qualitative-bankruptcy	0.652	0.694	0.645	0.500
servo	0.528	0.516	0.480	0.500
sleuth case1202	0.544	0.590	0.521	0.500
sleuth case2002	0.609	0.564	0.526	0.500
sleuth ex2015	0.589	0.599	0.733	0.500
sleuth ex2016	0.562	0.588	0.532	0.500
tae	0.544	0.592	0.533	0.500
teachingAssistant	0.533	0.528	0.499	0.500
veteran	0.520	0.520	0.502	0.500
white-clover	0.626	0.598	0.622	0.500
zoo	0.754	0.710	0.764	0.500
Overall	0.609 ± 0.097	0.593 ± 0.097	0.577 ± 0.096	0.500 ± 0.000

A.2.1. DETAILS FOR NN-MNAR

Description This pattern simulates a scenario where the propensity p_{ij} depends on the underlying matrix values X^* in an arbitrary manner. We achieve a comprehensive coverage of MNAR patterns by leveraging the expressiveness of neural networks.

Methodology One general form of MNAR can be described as follows: for all i and j , there exists some function f_{ij} on the true (hence unobserved) matrix X^* such that the propensity depends on X^* as follows: $p_{ij}(X^*) = \mathbb{P}(M_{ij} = 1 | X^*) = f_{ij}(X^*)$. By leveraging the expressiveness of neural networks, we propose a neural-net-based MAR pattern generator (NN-MNAR) that is designed to approximate arbitrary propensities characterized by functions f_{ij} .

Implementation Details For fixed indices i and j , NN-MNAR constructs the propensity p_{ij} in a two-step procedure. First, we randomly collect a subset of values from the matrix X^* and flatten them as a vector, say $X^*(i, j)$; we do this by first randomly generating a neighborhood $\mathbf{N}_{ij} \subset [m] \times [n]$, then the entries in the neighborhood $X^*_{st}, (s, t) \in \mathbf{N}_{ij}$ constitute the entries of the vector $X^*(i, j)$. Second, a neural-net function $g_{ij} : \mathbb{R}^{|\mathbf{N}_{ij}|} \rightarrow [0, 1]$ is constructed by randomly initializing the number of layers, depth, weight, and bias. At each training step, the random neighborhood \mathbf{N}_{ij} and the random neural-net g_{ij} collectively defines the propensity $p_{ij} = g_{ij}(X^*(i, j))$ from which MNAR missingness patterns are generated $M_{ij} \sim \text{Bern}(p_{ij})$.

A.2.2. DETAILS ON SEQ-MNAR

Description This pattern simulates a scenario where masking matrix values $M_{ij} \in \{0, 1\}$ for each column j are adaptively chosen depending on the information up to column $j - 1$ (i.e., regard columns as time). Specifically, we employ variants of bandit algorithms (Lattimore & Szepesvári, 2020) while regarding the binary masking matrix values as the two arms. Such patterns commonly arise in sequential experiments (Ghosh et al., 2024).

Methodology The true matrix X^* is transformed to constitute the reward. For each designated column j , one of the following bandit algorithm utilizes the all the information of X^* and M up to column $j - 1$ and chooses one of the two arms $\{0, 1\}$ via one of the following algorithms: ϵ -greedy, upper-confidence bound (UCB), Thompson-sampling (Thompson, 1933) or gradient bandit.

Implementation Details We generate exogenous Gaussian noise and add it to the true matrix X^* and regard X^* as the reward for arm 0 and its noisy version as the reward for arm 1. Then, starting from the first column with multiple rows as multiple agents, we randomly initiate (with random configurations) one of the four algorithms (Lattimore & Szepesvári, 2020): ϵ -greedy, Upper Confidence Bound (UCB) (Auer et al., 2002), Thompson sampling with random configurations (Thompson, 1933). Further, we have the option to randomly mix pooling techniques (Ghosh et al., 2024) on top of any of the four algorithms.

A.2.3. SELF-MNAR

Description: This pattern simulates a scenario where the probability of a value being missing is a direct function of the value itself. This pattern, commonly referred to as "self-masked MNAR", is widely utilized in the missing-data literature to model unbalanced class problems (Mohan, 2018; Sportisse et al., 2020b). A classic example occurs in income surveys, where individuals at the extremes of the income distribution, both very high and very low earners, are often less likely to disclose their income (Moore & Welniak, 2000). Similar patterns appear in other domains, such as substance use reporting or medical contexts where patients with severe symptoms might be less able to complete follow-up assessments (Ibrahim & Molenberghs, 2009).

Within the structured missingness taxonomy proposed by (Jackson et al., 2023), this mechanism is classified as **MNAR-UP** (Unstructured, Probabilistic). It is "Unstructured" because the missingness of an entry (i, j) is conditionally independent of the missingness status of other entries, and "Probabilistic" as it is determined by a probability function rather than a deterministic rule.

Methodology: For each designated target column j , the probability of an entry (i, j) being missing is determined by a logistic function of its value. The relationship is defined as $\mathbb{P}(M_{ij} = 0 | X^*_{ij}) = \sigma(\alpha \cdot X^*_{ij} + \beta_0)$ where $\sigma(z) = (1 + e^{-z})^{-1}$ is the sigmoid function.

Implementation Details: A random coefficient α is chosen from the set $\{-2, -1, 1, 2\}$ to introduce variability in the direction and magnitude of the value’s effect on its missingness probability. The bias term β_0 is calibrated to achieve a target missingness proportion, p .

A.2.4. CENSORING-MNAR

Description: This pattern models missingness arising from the physical limitations of measurement instruments, where values falling below a lower Limit of Detection or above an upper Limit of Quantification are not recorded. This results in left-censored or right-censored data, a common obstacle in environmental science, epidemiology, and biomedical research (Helsel, 2011; Chen et al., 2013). In fields like metabolomics and proteomics, this type of missingness is explicitly recognized as left-censored MNAR (Karpievitch et al., 2009; Lazar et al., 2016), as the probability of being missing is directly determined by the concentration falling below the detection threshold. Failing to appropriately account for this, or using simplistic substitution methods like replacing with zero, can introduce substantial bias. Modeling Censoring-MNAR is therefore essential for evaluating imputation methods on datasets generated by instrumentation with inherent sensitivity constraints.

Censoring-MNAR maps to the **MNAR-UD** (Unstructured, Deterministic) category in the structured missingness framework. It is "Unstructured" as the missingness of an entry is independent of other missingness indicators, and "Deterministic" because any value falling beyond the censoring threshold is missing with certainty.

Methodology: For each column j , a censoring direction (left or right) is chosen with equal probability. A cutoff value is determined based on a specified quantile, q_{censor} , of the set of currently observed (non-missing) values in that column. Let $X_{:,j}^*$ denote the set of observed values in column j , i.e., $X_{:,j}^* = \{X_{ij} \mid M_{ij} = 1\}$.

- **Left-Censoring:** All values in column j that are less than the q_{censor} -th quantile of the observed values in that same column are set to missing. The threshold is a single scalar value calculated from the column’s observed data.

$$M_{ij} = 0 \quad \text{if} \quad X_{ij} < \text{quantile}(X_{:,j}^*, q_{\text{censor}})$$

- **Right-Censoring:** All values in column j that are greater than the $(1 - q_{\text{censor}})$ -th quantile of the observed values in that column are set to missing. The threshold is a single scalar value.

$$M_{ij} = 0 \quad \text{if} \quad X_{ij} > \text{quantile}(X_{:,j}^*, 1 - q_{\text{censor}})$$

Implementation Details: The choice between left- and right-censoring is made randomly for each column with a probability of 0.5 for each. We introduce a hyperparameter q_{censor} for the censoring quantile that controls the fraction of data to be censored from either tail of the distribution. For our evaluation, we use $q_{\text{censor}} = 0.25$.

A.2.5. PANEL-MNAR

Description: This pattern simulates participant attrition (dropout) in longitudinal and panel data studies. This creates missingness where the dropout of a subject at a specific time point means all subsequent data for that subject is unobserved. Attrition is an inherent feature of long-term studies, including clinical trials and cohort studies (Little & Rubin, 2019; Van Buuren, 2012). The primary concern is "attrition bias," which arises when dropout is systematic—meaning those who leave the study differ significantly from those who remain (Hausman & Wise, 1979). This often constitutes an MNAR mechanism, particularly in clinical settings where patients might withdraw due to adverse effects or perceived lack of treatment efficacy, directly linking the dropout to the (unobserved) future outcomes (Ibrahim & Molenberghs, 2009; Little, 1995).

Methodology: The columns of the data matrix X^* are assumed to represent ordered time points $t = 0, 1, \dots, T - 1$. For each subject (row) i , a random dropout time $t_{0,i}$ is sampled. All observations for that subject from time $t_{0,i}$ onwards are masked as missing.

$$M_{ij} = 0 \quad \forall j \geq t_{0,i}$$

Implementation Details: For each row i , the dropout time $t_{0,i}$ is sampled uniformly from the range of possible time steps, i.e., $t_{0,i} \sim \text{Unif}\{1, \dots, T\}$.

A.2.6. POLARIZATION-MNAR

Description: This pattern simulates data where values falling in the middle of a feature’s distribution are preferentially removed, simulating survey non-response from individuals with moderate opinions. This is implemented by setting values between the q -th and $(1 - q)$ -th quantiles to missing. A ”soft” version makes the observation probability proportional to the value’s distance from the median. `Polarization-MNAR` is recognized in the survey methodology literature as a form of voluntary response bias or self-selection bias (Bethlehem, 2010). One obvious example can be found in online product reviews, which frequently exhibit a U-shaped or J-shaped distribution, heavily skewed towards the highest and lowest ratings while the middle ground remains sparse—sometimes referred to as the ”brag-and-moan” bias (Hu et al., 2009). Similarly, in political polling, nonresponse bias can be exacerbated if highly polarized individuals are more motivated to participate than moderates, potentially exaggerating measures of mass polarization (Cavari & Freedman, 2023).

This pattern maps to the ”Unstructured” MNAR categories of (Jackson et al., 2023). Specifically, our hard polarization variant, where values within a quantile range are missing with certainty, is an instance of **MNAR-UD** (Unstructured, Deterministic). Our soft polarization variant, where the missingness probability is a function of the value’s distance from the median, is an example of **MNAR-UP** (Unstructured, Probabilistic).

Hard Polarization Methodology: For each column j , values falling between two quantiles are deterministically masked. The quantiles are calculated using only the set of currently observed (non-’NaN’) values in that column. Let $X_{:,j}^*$ denote this set of observed values, i.e., $X_{:,j}^* = \{X_{ij} \mid M_{ij} = 1\}$. The lower and upper thresholds, L_j and H_j , are defined as:

$$L_j = \text{quantile}(X_{:,j}^*, q_{\text{thresh}})$$

$$H_j = \text{quantile}(X_{:,j}^*, 1 - q_{\text{thresh}})$$

An entry X_{ij} is then masked if its value falls between these two scalar thresholds:

$$M_{ij} = 0 \quad \text{if} \quad L_j < X_{ij} < H_j$$

Soft Polarization Methodology: The probability of a value being observed is made proportional to its normalized absolute distance from the column’s median, μ_j . This creates a softer, probabilistic version of the polarization effect. The missing probability is given by:

$$\mathbb{P}(M_{ij} = 0) = \epsilon + (1 - 2\epsilon) \frac{|X_{ij}^* - \mu_j|^\alpha}{\max_k (|X_{kj}^* - \mu_j|^\alpha)}$$

Implementation Details: For the hard polarization pattern, we introduce a hyperparameter q_{thresh} for the threshold quantile that defines the central portion of the distribution to be masked. For the soft polarization pattern, we have an exponent parameter α that controls the intensity of the polarization effect. Higher values of α make the observation probability more sensitive to deviations from the median. In the soft version, we also have a baseline probability ϵ that ensures even values at the median have a non-zero chance of being observed.

A.2.7. LATENT-FACTOR-MNAR

Description: This pattern generates a complex missingness structure where the probability of an entry being missing depends on unobserved (latent) characteristics of both its row and its column. This is most common in recommender systems and collaborative filtering, where the data (e.g., user ratings) are inherently MNAR (Marlin & Zemel, 2009; Steck, 2010). Users do not select items to rate uniformly; rather, their exposure to items and their decisions to provide a rating are strongly influenced by their underlying (latent) preferences—the very values the system aims to predict (Schnabel et al., 2016). This creates a selection bias where observed ratings are a biased sample of the full data. A standard approach in the literature assumes a low-rank structure for both the underlying data matrix and the missingness mechanism (propensity score matrix), implying they are governed by a shared set of latent factor (Sportisse et al., 2020a; Jin et al., 2022). Recent work in causal matrix completion explicitly models these latent confounders (Agarwal et al., 2023).

Methodology: The probability of an entry (i, j) being observed is modeled using a low-rank bilinear model. The observation probability is given by the sigmoid of a dot product of latent factors plus bias terms:

$$\mathbb{P}(M_{ij} = 1) = \sigma(u_i^T v_j + b_i + c_j)$$

where $u_i \in \mathbb{R}^k$ and $v_j \in \mathbb{R}^k$ are k -dimensional latent vectors for row i and column j , and b_i and c_j are scalar biases for the row and column, respectively.

Implementation Details: We specify the rank k that defines the dimensionality of the latent space, sampled as an integer. The elements of the latent factor matrices $U \in \mathbb{R}^{N \times k}$ and $V \in \mathbb{R}^{D \times k}$, and the bias vectors $b \in \mathbb{R}^N$ and $c \in \mathbb{R}^D$, are sampled independently from a standard normal distributions.

A.2.8. CLUSTER-MNAR

Description: This pattern induces missingness based on latent group-level characteristics. Rows and columns are first assigned to discrete clusters, and each cluster has a random effect that uniformly influences the observation probability of all its members. Such structures are prevalent in education (students clustered in schools), healthcare (patients clustered in hospitals), and cross-national surveys. In these settings, missing data patterns are often not independent across observations but rather clustered (Van Buuren, 2011). For example, in multi-center clinical trials or Cluster Randomized Trials, missingness can be heavily influenced by site-specific factors such as resource availability or staff training (Diaz-Ordaz et al., 2014). Ignoring this hierarchical structure during imputation fails to account for the within-cluster correlation and can lead to biased estimates (Enders et al., 2016). Because the missingness mechanism is related to these cluster-level effects, which may themselves be latent, the data is MNAR.

In the structured missingness taxonomy, we classify `Cluster-MNAR` as **MNAR-UP** (Unstructured, Probabilistic) due to the probabilistic dependence on unobserved factors, without dependence on other missingness indicators.

Methodology: The probability of an entry (i, j) being observed is determined by an additive model of random effects corresponding to the cluster assignments of its row i and column j . Denoting the row assignments by $C_R(i)$ and column assignments by $C_C(j)$, the observation probability is modeled as:

$$\mathbb{P}(M_{ij} = 1) = \sigma(g_{C_R(i)} + h_{C_C(j)} + \epsilon_{ij})$$

where:

- $\sigma(z) = (1 + e^{-z})^{-1}$ is the sigmoid function.
- $g_k \sim \mathcal{N}(0, \tau_r^2)$ is the random effect for row cluster k .
- $h_l \sim \mathcal{N}(0, \tau_c^2)$ is the random effect for column cluster l .
- $\epsilon_{ij} \sim \mathcal{N}(0, \epsilon_{\text{std}}^2)$ is an entry-specific noise term.

Implementation Details: For a matrix with N and D columns, row assignments $C_R(i)$ are drawn uniformly from $\{0, \dots, K_R - 1\}$ and column assignments $C_C(j)$ are drawn uniformly from $\{0, \dots, K_C - 1\}$, where K_R and K_C are the total number of row and column clusters, respectively. The number of row clusters K_R , the number of column clusters K_C , and the standard deviation of the random effects (τ_r , τ_c , ϵ_{std}) are hyperparameters specified for the data generation process.

A.2.9. TWO-PHASE-MNAR

Description: This pattern mimics multi-stage data collection, mirroring established methodologies such as "two-phase sampling" (or "double sampling") (Neyman, 1938) and "Planned Missing Data Designs" (Graham et al., 2006). These designs are frequently employed in large-scale surveys and epidemiological studies to manage costs and participant burden when certain variables are expensive or difficult to measure (Rhemtulla & Hancock, 2016). Another example includes market research where basic demographics are collected from all participants, but detailed purchasing behavior is only gathered from a subset, with missingness related to income level. In these designs, a full sample provides baseline information ("cheap" features), and a subset is strategically selected for follow-up ("expensive" features).

Methodology: Let $\mathcal{F} = \{0, 1, \dots, D - 1\}$ be the set of all column indices in the data matrix X . This set is randomly partitioned into a "cheap" subset $\mathcal{C} \subset \mathcal{F}$ and an "expensive" subset $\mathcal{E} \subset \mathcal{F}$, such that $\mathcal{C} \cup \mathcal{E} = \mathcal{F}$ and $\mathcal{C} \cap \mathcal{E} = \emptyset$. By design, features in the cheap set \mathcal{C} are always observed.

The decision to collect the expensive features for a given row i is based on a logistic model applied to its cheap features. Let $X_{i,\mathcal{C}}$ denote the vector of values $\{X_{ij} \mid j \in \mathcal{C}\}$ for row i . A score is calculated for each row:

$$s_i = \text{normalize}(X_{i,\mathcal{C}}^T w)$$

where w is a vector of random weights and the ‘normalize’ function applies z-score normalization to the resulting scores across all rows.

The probability that all expensive features are observed for row i is then given by:

$$\mathbb{P}(M_{ij} = 1 \text{ for all } j \in \mathcal{E}) = \sigma(\alpha + \beta \cdot s_i)$$

If the expensive features for row i are not observed (based on the probability above), then all of its values in the expensive columns are masked as missing, i.e., $M_{ij} = 1$ for all $j \in \mathcal{E}$.

Implementation Details: A fraction of columns, e.g., 50%, are randomly assigned to be ‘cheap’. The weight vector for the scoring model is sampled from a standard normal distribution, $w \sim \mathcal{N}(0, 1)$. Parameters α, β control the base rate and score-dependency of the observation probability. In our implementation, they are set to default values of $\alpha = 0$ and $\beta = 2.0$.

A.3. Ablation of Featurization and Pre-Training

To demonstrate the sources of TabImpute’s performance gains, we compare three variants: (i) Col-TabPFN method, (ii) EWF-TabPFN, which uses our entry-wise featurization with the original pre-trained TabPFN model, and (iii) TabImpute, which incorporates our synthetic pre-training pipeline. As shown in the full accuracy results table in Tab. 6, the entry-wise featurization leads to an improvement in overall accuracy scores from 0.561 to 0.860. Pre-training the model (i.e., TabImpute) on this task further increases the accuracy to 0.887, yielding gains across almost all missingness patterns. On top of this, TabImpute achieves this better accuracy with a much lower runtime: 1.986 ms per entry vs. EWF-TabPFN’s 4.110 ms per entry ($2.07\times$ faster).

A possible explanation for the effectiveness of entry-wise featurization is that it allows entry-specific information to route through the network without interference from other prediction targets, whereas Col-TabPFN entangles prediction routes. This role is analogous to how CLS tokens in BERT enable sentence-level information to be aggregated without interfering with token-level representations (Devlin et al., 2019).

A.4. Additional tables

Table 5. Other imputation methods

Name	Description
SoftImpute (Hastie et al., 2015)	Iterative soft thresholding singular value decomposition based on a low-rank assumption on the data.
k -Nearest Neighbors (Fix & Hodges, 1989)	Row-wise nearest neighbors mean. We set $k = 5$ for our tests.
HyperImpute (Jarrett et al., 2022)	Iterative imputation method optimizing over a suite of imputation methods.
Optimal transport method (Muzellec et al., 2020)	Uses optimal transport distances as a loss to impute missing values based on the principle that two randomly drawn batches from the same dataset should share similar data distributions.
MissForest (Stekhoven & Bühlmann, 2011)	Repeatedly trains a random forest model for each variable on the observed values to predict and fill in missing entries until convergence.
ICE (van Buuren & Groothuis-Oudshoorn, 2011)	Imputation with iterative and chained equations of linear/logistic models for conditional expectations.
MICE (Royston & White, 2011)	Handles missing data by iteratively imputing each incomplete variable using regression models that condition on all other variables.
GAIN (Yoon et al., 2018)	Adapts generative adversarial networks (Goodfellow et al., 2020) where the generator imputes missing values and the discriminator identifies which components are observed versus imputed.
MIWAE (Mattei & Frellsen, 2019)	Learns a deep latent variable model and then performs importance sampling for imputation.
ForestDiffusion (Jolicoeur-Martineau et al., 2024)	Trains a diffusion model using XGBoost directly on incomplete tabular data and then fills in missing values with an adapted inpainting algorithm.
TabPFN (Hollmann et al., 2023)	The <code>tabpfn-extensions</code> package includes a part to impute missing entries in a table column-by-column using TabPFN.
ReMasker (Du et al., 2023)	A transformer-based method using masked autoencoding.
CACTI (Gorla et al., 2025)	A transformer-based method that leverages copy-masking and leverages the text-based contextual information of column names. We use the version that does not use textual information (CMAE) to keep our tests fair.

Table 6. Imputation Accuracy \pm Standard Error by Missingness Pattern (All Methods)

Pattern	TabImpute	EWf-TabPFN	OT	HyperImpute	MissForest
MCAR	0.904 \pm 0.018	0.826 \pm 0.023	0.866 \pm 0.019	0.814 \pm 0.027	0.854 \pm 0.025
NN-MNAR	0.943 \pm 0.014	0.916 \pm 0.016	0.873 \pm 0.014	0.785 \pm 0.035	0.838 \pm 0.026
Self-MNAR	0.775 \pm 0.030	0.765 \pm 0.033	0.693 \pm 0.033	0.751 \pm 0.034	0.700 \pm 0.034
Col-MAR	0.921 \pm 0.018	0.888 \pm 0.014	0.788 \pm 0.032	0.868 \pm 0.029	0.830 \pm 0.025
Block-MNAR	0.937 \pm 0.013	0.923 \pm 0.014	0.857 \pm 0.027	0.854 \pm 0.027	0.850 \pm 0.024
Seq-MNAR	0.930 \pm 0.015	0.915 \pm 0.013	0.853 \pm 0.029	0.837 \pm 0.031	0.802 \pm 0.033
Panel-MNAR	0.955 \pm 0.008	0.889 \pm 0.019	0.918 \pm 0.011	0.883 \pm 0.031	0.897 \pm 0.019
Polarization-MNAR	0.825 \pm 0.025	0.896 \pm 0.020	0.787 \pm 0.021	0.631 \pm 0.039	0.580 \pm 0.033
Soft-Polarization-MNAR	0.805 \pm 0.047	0.867 \pm 0.022	0.773 \pm 0.029	0.669 \pm 0.036	0.625 \pm 0.039
Latent-Factor-MNAR	0.923 \pm 0.016	0.874 \pm 0.021	0.870 \pm 0.019	0.783 \pm 0.038	0.835 \pm 0.026
Cluster-MNAR	0.933 \pm 0.011	0.893 \pm 0.020	0.868 \pm 0.016	0.844 \pm 0.029	0.848 \pm 0.021
Two-Phase-MNAR	0.914 \pm 0.012	0.872 \pm 0.023	0.822 \pm 0.025	0.880 \pm 0.029	0.881 \pm 0.016
Censoring-MNAR	0.766 \pm 0.030	0.660 \pm 0.041	0.739 \pm 0.021	0.810 \pm 0.028	0.749 \pm 0.023
Overall	0.887 \pm 0.007	0.860 \pm 0.007	0.824 \pm 0.007	0.801 \pm 0.009	0.791 \pm 0.008

Pattern	K-NN	ICE	CACTI	SoftImpute	ForestDiffusion
MCAR	0.772 \pm 0.022	0.660 \pm 0.042	0.714 \pm 0.035	0.632 \pm 0.044	0.450 \pm 0.033
NN-MNAR	0.800 \pm 0.020	0.665 \pm 0.038	0.727 \pm 0.035	0.734 \pm 0.034	0.496 \pm 0.036
Self-MNAR	0.680 \pm 0.037	0.644 \pm 0.052	0.652 \pm 0.041	0.511 \pm 0.044	0.662 \pm 0.036
Col-MAR	0.872 \pm 0.017	0.845 \pm 0.034	0.806 \pm 0.024	0.720 \pm 0.030	0.511 \pm 0.038
Block-MNAR	0.893 \pm 0.014	0.806 \pm 0.032	0.752 \pm 0.045	0.850 \pm 0.027	0.740 \pm 0.030
Seq-MNAR	0.851 \pm 0.027	0.784 \pm 0.037	0.780 \pm 0.033	0.758 \pm 0.042	0.603 \pm 0.030
Panel-MNAR	0.940 \pm 0.011	0.819 \pm 0.039	0.875 \pm 0.025	0.671 \pm 0.043	0.661 \pm 0.040
Polarization-MNAR	0.658 \pm 0.028	0.566 \pm 0.041	0.511 \pm 0.031	0.651 \pm 0.048	0.291 \pm 0.042
Soft-Polarization-MNAR	0.635 \pm 0.035	0.681 \pm 0.037	0.561 \pm 0.040	0.719 \pm 0.034	0.749 \pm 0.033
Latent-Factor-MNAR	0.810 \pm 0.022	0.719 \pm 0.042	0.772 \pm 0.027	0.724 \pm 0.038	0.584 \pm 0.030
Cluster-MNAR	0.807 \pm 0.018	0.744 \pm 0.044	0.742 \pm 0.034	0.672 \pm 0.045	0.579 \pm 0.035
Two-Phase-MNAR	0.905 \pm 0.015	0.875 \pm 0.028	0.858 \pm 0.031	0.691 \pm 0.044	0.575 \pm 0.040
Censoring-MNAR	0.561 \pm 0.045	0.795 \pm 0.036	0.721 \pm 0.036	0.448 \pm 0.049	0.738 \pm 0.039
Overall	0.783 \pm 0.009	0.739 \pm 0.011	0.729 \pm 0.010	0.675 \pm 0.012	0.588 \pm 0.011

Pattern	ReMasker	Col-TabPFN	MIWAE	MICE	GAIN
MCAR	0.647 \pm 0.032	0.448 \pm 0.043	0.276 \pm 0.046	0.350 \pm 0.046	0.556 \pm 0.040
NN-MNAR	0.397 \pm 0.046	0.546 \pm 0.043	0.366 \pm 0.051	0.360 \pm 0.050	0.507 \pm 0.040
Self-MNAR	0.570 \pm 0.055	0.396 \pm 0.046	0.391 \pm 0.045	0.534 \pm 0.057	0.557 \pm 0.054
Col-MAR	0.662 \pm 0.046	0.575 \pm 0.050	0.513 \pm 0.047	0.477 \pm 0.053	0.355 \pm 0.057
Block-MNAR	0.685 \pm 0.045	0.651 \pm 0.046	0.661 \pm 0.028	0.537 \pm 0.038	0.217 \pm 0.051
Seq-MNAR	0.540 \pm 0.045	0.646 \pm 0.046	0.552 \pm 0.045	0.423 \pm 0.048	0.258 \pm 0.044
Panel-MNAR	0.681 \pm 0.051	0.340 \pm 0.049	0.498 \pm 0.051	0.471 \pm 0.048	0.493 \pm 0.053
Polarization-MNAR	0.378 \pm 0.043	0.908 \pm 0.030	0.625 \pm 0.027	0.224 \pm 0.038	0.329 \pm 0.042
Soft-Polarization-MNAR	0.417 \pm 0.056	0.682 \pm 0.043	0.605 \pm 0.033	0.262 \pm 0.039	0.502 \pm 0.060
Latent-Factor-MNAR	0.462 \pm 0.047	0.581 \pm 0.049	0.428 \pm 0.047	0.368 \pm 0.051	0.386 \pm 0.048
Cluster-MNAR	0.516 \pm 0.053	0.596 \pm 0.047	0.433 \pm 0.049	0.356 \pm 0.046	0.427 \pm 0.046
Two-Phase-MNAR	0.736 \pm 0.049	0.529 \pm 0.047	0.538 \pm 0.043	0.530 \pm 0.049	0.249 \pm 0.049
Censoring-MNAR	0.673 \pm 0.050	0.397 \pm 0.044	0.368 \pm 0.047	0.554 \pm 0.049	0.445 \pm 0.054
Overall	0.567 \pm 0.014	0.561 \pm 0.014	0.481 \pm 0.013	0.419 \pm 0.014	0.406 \pm 0.014

Table 7. Mean Column-wise 1-Wasserstein Distance \pm Standard Error by Missingness Pattern

Pattern	ICE	HyperImpute	MissForest	K-NN	MICE
MCAR	0.941 \pm 0.012	0.919 \pm 0.019	0.823 \pm 0.019	0.735 \pm 0.018	0.812 \pm 0.033
NN-MNAR	0.916 \pm 0.020	0.922 \pm 0.020	0.862 \pm 0.020	0.740 \pm 0.023	0.830 \pm 0.030
Self-MNAR	0.790 \pm 0.033	0.727 \pm 0.036	0.655 \pm 0.035	0.620 \pm 0.033	0.741 \pm 0.052
Seq-MNAR	0.833 \pm 0.025	0.848 \pm 0.020	0.818 \pm 0.019	0.794 \pm 0.021	0.854 \pm 0.028
Polarization-MNAR	0.662 \pm 0.037	0.689 \pm 0.040	0.579 \pm 0.041	0.744 \pm 0.032	0.371 \pm 0.047
Soft-Polarization-MNAR	0.809 \pm 0.037	0.786 \pm 0.039	0.783 \pm 0.041	0.628 \pm 0.042	0.551 \pm 0.043
Latent-Factor-MNAR	0.934 \pm 0.016	0.917 \pm 0.022	0.875 \pm 0.020	0.748 \pm 0.021	0.833 \pm 0.031
Cluster-MNAR	0.918 \pm 0.019	0.913 \pm 0.021	0.836 \pm 0.021	0.756 \pm 0.020	0.828 \pm 0.035
Two-Phase-MNAR	0.832 \pm 0.030	0.797 \pm 0.030	0.760 \pm 0.023	0.838 \pm 0.019	0.769 \pm 0.041
Overall	0.848 \pm 0.010	0.835 \pm 0.010	0.777 \pm 0.010	0.734 \pm 0.009	0.732 \pm 0.015
Pattern	ForestDiffusion	OT	TabImpute	CACTI	EWf-TabPFN
MCAR	0.819 \pm 0.021	0.715 \pm 0.017	0.720 \pm 0.029	0.659 \pm 0.037	0.508 \pm 0.036
NN-MNAR	0.777 \pm 0.018	0.724 \pm 0.021	0.712 \pm 0.033	0.707 \pm 0.041	0.578 \pm 0.038
Self-MNAR	0.679 \pm 0.034	0.551 \pm 0.030	0.656 \pm 0.035	0.611 \pm 0.040	0.625 \pm 0.038
Seq-MNAR	0.909 \pm 0.017	0.745 \pm 0.020	0.635 \pm 0.029	0.681 \pm 0.035	0.588 \pm 0.039
Polarization-MNAR	0.350 \pm 0.048	0.876 \pm 0.023	0.885 \pm 0.019	0.592 \pm 0.037	0.878 \pm 0.025
Soft-Polarization-MNAR	0.597 \pm 0.037	0.720 \pm 0.036	0.675 \pm 0.043	0.675 \pm 0.040	0.781 \pm 0.032
Latent-Factor-MNAR	0.765 \pm 0.025	0.727 \pm 0.022	0.695 \pm 0.034	0.726 \pm 0.031	0.552 \pm 0.044
Cluster-MNAR	0.786 \pm 0.024	0.728 \pm 0.021	0.687 \pm 0.034	0.732 \pm 0.032	0.572 \pm 0.045
Two-Phase-MNAR	0.907 \pm 0.025	0.683 \pm 0.028	0.746 \pm 0.028	0.821 \pm 0.035	0.643 \pm 0.041
Overall	0.732 \pm 0.013	0.719 \pm 0.009	0.712 \pm 0.011	0.689 \pm 0.013	0.636 \pm 0.014
Pattern	ReMasker	SoftImpute	MIWAE	GAIN	Col-TabPFN
MCAR	0.805 \pm 0.026	0.464 \pm 0.058	0.407 \pm 0.021	0.595 \pm 0.033	0.049 \pm 0.017
NN-MNAR	0.659 \pm 0.055	0.479 \pm 0.063	0.466 \pm 0.029	0.554 \pm 0.038	0.140 \pm 0.041
Self-MNAR	0.501 \pm 0.054	0.406 \pm 0.047	0.283 \pm 0.038	0.502 \pm 0.054	0.214 \pm 0.036
Seq-MNAR	0.515 \pm 0.048	0.636 \pm 0.048	0.596 \pm 0.029	0.259 \pm 0.041	0.302 \pm 0.043
Polarization-MNAR	0.398 \pm 0.044	0.675 \pm 0.042	0.709 \pm 0.034	0.392 \pm 0.050	0.757 \pm 0.034
Soft-Polarization-MNAR	0.297 \pm 0.054	0.645 \pm 0.040	0.613 \pm 0.041	0.494 \pm 0.061	0.453 \pm 0.046
Latent-Factor-MNAR	0.634 \pm 0.048	0.507 \pm 0.060	0.502 \pm 0.033	0.430 \pm 0.044	0.198 \pm 0.043
Cluster-MNAR	0.639 \pm 0.054	0.436 \pm 0.062	0.496 \pm 0.031	0.457 \pm 0.041	0.185 \pm 0.043
Two-Phase-MNAR	0.656 \pm 0.050	0.596 \pm 0.046	0.563 \pm 0.038	0.171 \pm 0.044	0.408 \pm 0.039
Overall	0.567 \pm 0.018	0.538 \pm 0.018	0.515 \pm 0.013	0.428 \pm 0.017	0.301 \pm 0.016

Table 8. Mean Column-wise $R^2 \pm$ Standard Deviation by Missingness Pattern

Pattern	EWf-TabPFN	TabImpute	HyperImpute	ICE	MissForest
MCAR	0.395 \pm 0.036	0.414 \pm 0.035	0.409 \pm 0.035	0.387 \pm 0.035	0.401 \pm 0.036
NN-MNAR	0.387 \pm 0.035	0.382 \pm 0.034	0.364 \pm 0.034	0.348 \pm 0.033	0.351 \pm 0.033
Self-MNAR	0.297 \pm 0.039	0.285 \pm 0.039	0.234 \pm 0.038	0.250 \pm 0.037	0.207 \pm 0.030
Col-MAR	0.308 \pm 0.033	0.289 \pm 0.035	0.285 \pm 0.034	0.287 \pm 0.034	0.242 \pm 0.032
Block-MNAR	0.283 \pm 0.032	0.256 \pm 0.033	0.242 \pm 0.034	0.229 \pm 0.033	0.221 \pm 0.033
Seq-MNAR	0.234 \pm 0.030	0.218 \pm 0.027	0.246 \pm 0.029	0.234 \pm 0.030	0.210 \pm 0.028
Panel-MNAR	0.275 \pm 0.028	0.290 \pm 0.029	0.285 \pm 0.027	0.271 \pm 0.029	0.271 \pm 0.028
Polarization-MNAR	0.230 \pm 0.022	0.190 \pm 0.019	0.189 \pm 0.020	0.177 \pm 0.021	0.156 \pm 0.017
Soft-Polarization-MNAR	0.177 \pm 0.027	0.148 \pm 0.024	0.146 \pm 0.024	0.137 \pm 0.023	0.131 \pm 0.022
Latent-Factor-MNAR	0.347 \pm 0.034	0.338 \pm 0.033	0.335 \pm 0.034	0.331 \pm 0.033	0.322 \pm 0.034
Cluster-MNAR	0.350 \pm 0.036	0.342 \pm 0.035	0.342 \pm 0.037	0.325 \pm 0.036	0.325 \pm 0.036
Two-Phase-MNAR	0.370 \pm 0.035	0.331 \pm 0.037	0.333 \pm 0.037	0.334 \pm 0.036	0.310 \pm 0.034
Censoring-MNAR	0.177 \pm 0.025	0.143 \pm 0.020	0.121 \pm 0.019	0.125 \pm 0.019	0.097 \pm 0.017
Overall	0.295 \pm 0.009	0.279 \pm 0.009	0.272 \pm 0.009	0.264 \pm 0.009	0.249 \pm 0.009

Pattern	OT	CACTI	K-NN	MICE	GAIN
MCAR	0.401 \pm 0.034	0.337 \pm 0.037	0.323 \pm 0.036	0.302 \pm 0.036	0.318 \pm 0.031
NN-MNAR	0.334 \pm 0.033	0.263 \pm 0.036	0.278 \pm 0.031	0.254 \pm 0.033	0.265 \pm 0.026
Self-MNAR	0.211 \pm 0.034	0.203 \pm 0.032	0.207 \pm 0.033	0.264 \pm 0.044	0.224 \pm 0.029
Col-MAR	0.221 \pm 0.031	0.242 \pm 0.030	0.227 \pm 0.032	0.182 \pm 0.030	0.156 \pm 0.027
Block-MNAR	0.199 \pm 0.029	0.179 \pm 0.031	0.186 \pm 0.029	0.155 \pm 0.027	0.098 \pm 0.016
Seq-MNAR	0.192 \pm 0.023	0.186 \pm 0.032	0.213 \pm 0.027	0.139 \pm 0.023	0.099 \pm 0.015
Panel-MNAR	0.247 \pm 0.025	0.243 \pm 0.029	0.277 \pm 0.028	0.146 \pm 0.021	0.167 \pm 0.023
Polarization-MNAR	0.177 \pm 0.018	0.150 \pm 0.019	0.146 \pm 0.018	0.109 \pm 0.015	0.109 \pm 0.013
Soft-Polarization-MNAR	0.108 \pm 0.020	0.114 \pm 0.022	0.075 \pm 0.018	0.066 \pm 0.016	0.078 \pm 0.014
Latent-Factor-MNAR	0.306 \pm 0.031	0.253 \pm 0.033	0.246 \pm 0.031	0.227 \pm 0.032	0.202 \pm 0.023
Cluster-MNAR	0.314 \pm 0.033	0.280 \pm 0.035	0.254 \pm 0.032	0.225 \pm 0.032	0.239 \pm 0.029
Two-Phase-MNAR	0.260 \pm 0.030	0.285 \pm 0.036	0.293 \pm 0.031	0.191 \pm 0.030	0.198 \pm 0.026
Censoring-MNAR	0.084 \pm 0.016	0.103 \pm 0.012	0.095 \pm 0.011	0.131 \pm 0.022	0.127 \pm 0.020
Overall	0.235 \pm 0.009	0.218 \pm 0.009	0.217 \pm 0.008	0.184 \pm 0.008	0.175 \pm 0.007

Pattern	ReMasker	SoftImpute	ForestDiffusion	Col-TabPFN	MIWAE
MCAR	0.327 \pm 0.036	0.265 \pm 0.041	0.220 \pm 0.029	0.070 \pm 0.008	0.036 \pm 0.005
NN-MNAR	0.196 \pm 0.032	0.223 \pm 0.043	0.177 \pm 0.026	0.042 \pm 0.006	0.025 \pm 0.003
Self-MNAR	0.151 \pm 0.026	0.166 \pm 0.030	0.116 \pm 0.024	0.106 \pm 0.016	0.026 \pm 0.004
Col-MAR	0.185 \pm 0.032	0.167 \pm 0.033	0.108 \pm 0.020	0.081 \pm 0.011	0.030 \pm 0.003
Block-MNAR	0.149 \pm 0.031	0.165 \pm 0.035	0.106 \pm 0.017	0.051 \pm 0.008	0.023 \pm 0.003
Seq-MNAR	0.111 \pm 0.021	0.181 \pm 0.032	0.089 \pm 0.014	0.034 \pm 0.003	0.022 \pm 0.003
Panel-MNAR	0.186 \pm 0.027	0.181 \pm 0.032	0.120 \pm 0.016	0.083 \pm 0.011	0.039 \pm 0.006
Polarization-MNAR	0.119 \pm 0.019	0.118 \pm 0.021	0.091 \pm 0.012	0.036 \pm 0.004	0.029 \pm 0.004
Soft-Polarization-MNAR	0.046 \pm 0.012	0.077 \pm 0.021	0.031 \pm 0.004	0.004 \pm 0.001	0.014 \pm 0.001
Latent-Factor-MNAR	0.177 \pm 0.029	0.194 \pm 0.039	0.152 \pm 0.022	0.053 \pm 0.007	0.028 \pm 0.003
Cluster-MNAR	0.212 \pm 0.034	0.187 \pm 0.038	0.181 \pm 0.027	0.058 \pm 0.009	0.033 \pm 0.005
Two-Phase-MNAR	0.263 \pm 0.038	0.190 \pm 0.035	0.126 \pm 0.022	0.086 \pm 0.012	0.022 \pm 0.003
Censoring-MNAR	0.080 \pm 0.012	0.081 \pm 0.021	0.071 \pm 0.011	0.072 \pm 0.018	0.067 \pm 0.018
Overall	0.169 \pm 0.008	0.169 \pm 0.009	0.122 \pm 0.006	0.060 \pm 0.003	0.030 \pm 0.002

Table 9. Mean Normalized Negative RMSE \pm Standard Error by Missingness Pattern including a nonlinear factor model-based TabImpute. Note that these normalized values are slightly different than Tab. 1 because the nonlinear model is included here.

Pattern	TabImpute	HyperImpute	TabImpute _{Nonlinear}	MissForest
MCAR	0.880 \pm 0.021	0.803 \pm 0.031	0.835 \pm 0.022	0.866 \pm 0.022
NN-MNAR	0.898 \pm 0.019	0.758 \pm 0.036	0.835 \pm 0.022	0.816 \pm 0.029
Self-MNAR	0.705 \pm 0.037	0.689 \pm 0.039	0.613 \pm 0.043	0.639 \pm 0.041
Col-MAR	0.868 \pm 0.030	0.806 \pm 0.040	0.836 \pm 0.029	0.764 \pm 0.038
Block-MNAR	0.890 \pm 0.026	0.873 \pm 0.027	0.868 \pm 0.029	0.860 \pm 0.023
Seq-MNAR	0.919 \pm 0.015	0.863 \pm 0.030	0.890 \pm 0.018	0.828 \pm 0.031
Panel-MNAR	0.893 \pm 0.027	0.847 \pm 0.034	0.448 \pm 0.063	0.891 \pm 0.022
Polarization-MNAR	0.800 \pm 0.024	0.619 \pm 0.039	0.751 \pm 0.030	0.564 \pm 0.032
Soft-Polarization-MNAR	0.756 \pm 0.045	0.709 \pm 0.034	0.808 \pm 0.034	0.665 \pm 0.041
Latent-Factor-MNAR	0.888 \pm 0.020	0.773 \pm 0.035	0.857 \pm 0.020	0.832 \pm 0.024
Cluster-MNAR	0.896 \pm 0.016	0.833 \pm 0.029	0.858 \pm 0.017	0.824 \pm 0.022
Two-Phase-MNAR	0.879 \pm 0.026	0.859 \pm 0.031	0.871 \pm 0.026	0.867 \pm 0.020
Censoring-MNAR	0.711 \pm 0.032	0.790 \pm 0.039	0.623 \pm 0.039	0.673 \pm 0.036
Overall	0.845 \pm 0.008	0.786 \pm 0.010	0.776 \pm 0.010	0.776 \pm 0.009

Table 10. Synthetic Data Generation Parameters

Missingness Pattern	Parameter Name	Symbol	Value
MCAR	Missing probability	p	0.4
Col-MAR	Missing probability	p	0.4
NN-MNAR	Neighborhood size	$ N_{ij} $	Variable
	Network layers	L	Random
	Network depth	d	Random
	Weight initialization	W	Random
	Bias initialization	b	Random
Self-MNAR	Coefficient set	α	$\{-2, -1, 1, 2\}$
	Target missing proportion	$p_{missing}$	Variable
Block-MNAR	Missing probability	p	0.4
	Matrix size N	N	100
	Matrix size T	T	50
	Row blocks	B_r	10
	Column blocks	B_c	10
	Convolution type	-	mean
Seq-MNAR	Missing probability	p	0.4
	Algorithm	-	epsilon_greedy
	Pooling	-	False
	Epsilon	ϵ	0.4
	Epsilon decay	γ	0.99
	Random seed	s	42
Panel-MNAR	No explicit hyperparameters (dropout time sampled uniformly)		
Polarization-MNAR	Threshold quantile	q_{thresh}	0.25
Soft-Polarization-MNAR	Polarization alpha	α	2.5
	Polarization epsilon	ϵ	0.05
Latent-Factor-MNAR	Latent rank (low)	k_{low}	1
	Latent rank (high)	k_{high}	5
Cluster-MNAR	Number of row clusters	K_R	5
	Number of column clusters	K_C	4
Two-Phase-MNAR	Cheap feature fraction	f_{cheap}	0.4
Censoring-MNAR	Censoring quantile	q_{censor}	0.25

Table 11. OpenML datasets

Dataset	Size	Domain	Description
EgyptianSkulls	150 × 5	Anthropology	Cranial measurements over time in Egypt
humans_numeric	75 × 15	Biology	Human body measurements
FacultySalaries	50 × 5	Education/Economics	University faculty salary data
SMSA	59 × 16	Demographics/Economics	U.S. metropolitan statistical area data
Student-Scores	56 × 13	Education	Student exam scores
analcatsdata_election2000	67 × 15	Political science	2000 U.S. presidential election results
analcatsdata_gviolence	74 × 9	Criminology	Gun violence statistics
analcatsdata_olympic2000	66 × 12	Sports/Economics	Olympic results and country stats
basketball	96 × 5	Sports analytics	Basketball performance data
visualizing_hamster	73 × 6	Education/Toy	Example dataset for teaching
witmer_census_1980	50 × 5	Demographics	U.S. census microdata (1980)
MercuryinBass	53 × 10	Environmental chemistry	Mercury concentrations in fish
SolarPower	204 × 5	Energy/Engineering	Solar power output records
WineDataset	178 × 14	Chemistry/Oenology	Wine physicochemical properties
alcohol-qcm-sensor	125 × 15	Analytical chemistry	Alcohol detection sensor readings
benzo32	195 × 33	Chemistry/Toxicology	Benzodiazepine compound data
machine_cpu	209 × 7	Computer systems	Predicting CPU performance
pwLinear	200 × 11	Mathematics/Engineering	Piecewise linear regression benchmark
pyrim	74 × 28	Chemistry/Pharmacology	Pyrimethamine bioassay compounds
slump	103 × 10	Civil engineering	Concrete slump test properties
ICU	200 × 20	Medicine	Intensive care patient data
appendicitis_test	106 × 8	Medicine	Appendicitis diagnosis
appendicitis_test_edsa	106 × 8	Medicine	Educational appendicitis dataset
breast-cancer-coimbra	116 × 10	Medicine	Breast cancer diagnosis data
Rainfall-in-Kerala-1901-2017	117 × 18	Climate science	Rainfall time series in Kerala
pollution	60 × 16	Environmental science	Air pollution measurements
treepit	86 × 10	Ecology	Bird habitat distribution
autoPrice	159 × 16	Business/Economics	Automobile pricing dataset
dataset_analcatsdata_creditscore	100 × 7	Finance	Credit scoring dataset
Swiss-banknote-conterfeit-detection	200 × 7	Finance/Fraud	Banknote authenticity classification
Glass-Classification	214 × 10	Forensics/Materials	Glass chemical composition (forensics)
chatfield_4	235 × 13	Statistics/Time series	Textbook time series data (Chatfield)
chscase_vine1	52 × 10	Agriculture/Statistics	Vine growth study
edm	154 × 18	Education	Student learning performance
metafeatures	75 × 32	Meta-learning	Dataset-level features
rabe_131	50 × 6	Chemistry/Benchmark	Spectroscopy regression dataset
rabe_148	66 × 6	Chemistry/Benchmark	Spectroscopy regression dataset
rabe_265	51 × 7	Chemistry/Benchmark	Spectroscopy regression dataset
sleuth_case1201	50 × 7	Statistics/Education	Applied regression textbook data
sleuth_ex1605	62 × 6	Statistics/Education	Applied regression textbook data
wisconsin	194 × 33	Medicine	Wisconsin breast cancer dataset

Table 12. Non-normalized RMSE Values for MCAR (Probability of Missing = 0.4) by Dataset

Dataset	TabImpute	EWf-TabPFN	HyperImpute	MissForest	OT
EgyptianSkulls	0.995	1.019	1.057	1.047	1.074
FacultySalaries	0.605	0.795	0.720	0.615	0.638
Glass-Classification	0.865	0.900	0.834	0.864	0.842
ICU	1.006	0.992	1.080	1.057	0.993
MercuryinBass	0.768	0.870	0.846	0.791	0.808
Rainfall-in-Kerala-1901-2017	0.876	0.918	0.855	0.929	0.924
SMSA	0.941	0.911	1.069	0.893	0.935
SolarPower	0.876	0.785	0.862	0.878	0.907
Student-Scores	0.431	0.441	0.425	0.471	0.520
Swiss-banknote-conterfeit-detection	0.731	0.926	0.805	0.664	0.732
WineDataset	0.760	0.866	0.738	0.732	0.723
alcohol-qcm-sensor	0.358	0.449	0.408	0.392	0.504
analcadata_election2000	0.738	2.969	3.454	5.660	5.869
analcadata_gviolence	0.757	0.812	0.873	0.940	0.826
analcadata_olympic2000	0.622	0.550	0.600	0.587	0.617
appendicitis_test	0.631	0.787	0.588	0.726	0.692
appendicitis_test_edsa	0.591	0.735	0.610	0.660	0.653
autoPrice	0.631	0.735	0.657	0.618	0.646
basketball	0.969	0.995	1.063	1.074	0.987
benzo32	1.019	1.003	1.001	1.000	0.889
breast-cancer-coimbra	0.937	0.913	1.068	0.964	0.939
chatfield_4	0.421	0.480	0.480	0.444	0.476
chscase_vine1	0.809	0.692	0.885	0.746	0.841
dataset_analcadata_creditscore	1.172	1.006	1.084	1.069	1.006
divorce_prediction	0.510	0.480	0.484	0.433	0.458
edm	0.602	0.767	0.536	0.555	0.561
humans_numeric	0.966	1.004	0.985	0.994	1.014
machine_cpu	0.779	0.927	0.824	0.729	0.818
metafeatures	1.437	2.471	3.294	4.329	3.578
pollution	0.941	0.905	1.087	0.871	0.911
pwLinear	0.999	1.038	1.310	1.311	1.058
pyrim	0.732	0.802	0.666	0.678	0.761
rabe_131	0.966	0.636	0.944	0.986	0.926
rabe_148	0.828	0.856	1.232	0.953	0.984
rabe_265	1.033	1.060	1.169	1.017	1.007
sleuth_case1201	0.834	0.943	0.862	0.891	0.895
sleuth_ex1605	0.973	1.045	1.144	1.026	0.932
slump	0.835	0.954	0.737	0.894	0.874
treepit	0.980	1.044	0.909	0.907	0.917
visualizing_hamster	0.817	0.921	1.019	0.821	0.849
wisconsin	0.731	0.645	0.555	0.661	0.702
witmer_census_1980	0.906	0.988	0.864	0.894	0.898